Thesis in pharmacology for the degree *candidatus pharmaciæ*

Block of neuronal nicotinic receptors by NMDA receptor antagonists

Screening inhibitors with fluorescent probes

by

Bjørn Oddvar Strøm

Department of Pharmaceutical biosciences

School of Pharmacy

Faculty of Mathematics and Natural Sciences

University of Oslo

Oslo, October 2006

FOREWORD

The work on this master thesis in pharmacology was done at the Norwegian Defence Research Establishment (FFI), Department for Protection, Kjeller, from November 2005 to October 2006. The thesis is part of the degree *cand. pharm.* at the school of pharmacy at the University of Oslo.

Most of all, I would like to thank my advisor at FFI, Dr. Avi Ring for his enthusiasm and for all the advice, help and encouragement throughout this year. I do not think anyone could wish for a better advisor!

I would also like my advisor at the School of Pharmacy, Professor Ragnhild Paulsen, for much helpful advice and valuable comments on the manuscript.

A large thanks goes to Rita Tansø for training and looking after me in the lab, and always being of great help when I needed it. I would also like to thank you for preparing the astrocytes.

I would like to thank everyone at Porton Down, in particular Dr. John Tattersall for scientific guidance and Simon Turner, for making my stay in England a great experience, both in and out of the lab. I would also like to thank UNIFOR and FFI for financing my stay in England.

I would like to thank the Norwegian Defence Reasearch Establishment for providing the equipment and resources to make this thesis possible.

I thank Baufort Ipsen in Paris, France for the gift of gacyclidine.

I would like to thank everybody at “nybygget” for making it a truly great place to be. Thank you for all the nice conversations and all the encouragement. I hope I will stay in touch with all of you.

Eirin, it has been great sharing the office with you this past year and to get to know you better. Thank you for all the conversations, laughs, meals and all the good times.

I would also like to thank Eirin, Ingvild and Håvard for proof-reading my thesis. The remaining mistakes are all mine.

Finally I would like to thank my family and friends for their great support and patience. I am looking forward to seeing more of you all!

Kjeller, October 2006

Bjørn Oddvar Strøm

TABLE OF CONTENTS

ABSTRACT

Neuronal nicotinic acetylcholine receptors (nAChRs) are implicated in several diseases of the central nervous system, including Alzheimer's and Parkinson's diseases. They play a role in modulating release of neurotransmittors and in the development and intervention of brain seizures and neurodegeneration caused by organophosphate poisoning, a major lethal threat in developing countries.

A method was developed to screen drugs for effects on nAChR. The method uses the ratiometric Ca^{2+}-probe fura-2 to measure, with the aid of a plate reader, nicotine induced responses in the human neuroblastoma cell line SH-SY5Y. The method was validated using published data for the Alzheimer drug memantine.

Drugs that show effects against tremor and brain seizures were characterised, including the Parkinson drugs biperiden, procyclidine, and trihexphenidyl. These drugs all blocked nAChR with an IC_{50} in a narrow range from 0.75 μM to 1.5 μM. The potencies of the drugs at the nAChR were greater than at the NMDA receptors, implicating a relevance of drug effects on nAChR in the mechanisms of inhibition of seizures. The nAChR block of the drugs were use- and voltage-dependent, features particularly suitable for a drug used to restrain epileptogenic seizures. Caramiphen, a potent antagonist at muscarinic acetylcholine receptors, also blocks nAChR with an IC_{50} of 0.3 μM.

The novel NMDA-receptor blocker gacyclidine (GK11) was shown to block the nAChR with an IC_{50} of 0.3 μM for its racemate and 0.16 μM for the pure (-)-isomer. The novel finding that gacyclidine blocks nAChR makes this receptor a good candidate for the "non-NMDA" binding sites that have been established, but not yet identified, for gacycyclidine.

Several novel bis-quarternary pyridine compounds inhibited nAChR with IC_{50} values inversely correlated with the length of the carbon chain linker, differing from the relative potencies of the drugs at muscle nAChR. This finding is, because of ganglionic blockade, highly relevant in selecting a suitable candidate to combat organophosphate poisoning.

ABBREVIATIONS

ACh	Acetylcholine
AChE	Acetylcholine esterase
AD	Alzheimer's disease
AMP	Adenosine monophosphate
ATP	Adenosine trisphosphate
$[Ca^{2+}]_i$	Intracellular calcium concentration
CAM	Calmodulin
cAMP	cyclic AMP
CCD	Charge coupled device
CICR	Calcium induced calcium release
CNS	Central nervous system
DMSO	Dimethyl sulfoxide
DSTL	Defence Science and Technology Laboratories
EC_{50}	Concentration giving 50% of the maximal cellular response
ED_{50}	Effective dose in 50% of the tested animals
EDTA	Ethylenediaminetetraacetic acid
ER	Endoplasmatic reticulum
FBS	Foetal Bovine Serum
G	Gravitational Force
HS	Horse Serum
IC_{50}	Concentration inhibiting 50% of the maximal cellular response
IP_3	Inositol 1,4,5 triphosphate
K_d	Effective dissociation constant
mAChR	Muscarinic acetylcholine receptor
nAChR	Nicotinic acetylcholine receptor
NMDA	N-methyl-D-aspartate
NMDA-R	NMDA receptor
OP	Organophosphate
PBS	Phosphate Buffered Saline
PD	Parkinson's disease

PMCA	Plasma-membrane Ca^{2+}-ATPase
ROS	Reactive oxygen species
SE	Standard Error
SEM	Standard Error of the Mean
SERCA	Sarco/endoplasmatic Ca^{2+} ATPase
UV	Ultra violet
VOCC	Voltage Operated Ca^{2+}-channels

1 INTRODUCTION

1.1 Background

Acetylcholine (ACh) is a major neurotransmitter both in the central and the peripheral nervous system. There are two distinct classes of ACh receptors; ligand gated ion channels and metabotropic receptors, called nicotinic and muscarinic acetylcholine receptors respectively (nAChR and mAChR), due their sensitivity to the plant alkaloids nicotine and muscarine (Taylor and Brown 2006).

Neuronal nAChRs are found throughout the central nervous system (CNS). They are thought to have mainly modulatory functions on neurons. Presynaptically they modulate the release of different neurotransmittors. They are also present post-synaptically, but to a lesser degree. (Gotti *et al.* 2006a).

Many drugs used in the treatment of CNS disorders target glutamatergic receptors and mAChRs. Some also have effects on nAChR, although these are not well characterised. Amongst these are anti-cholinergic Parkinson drugs and possible countermeasure agents to organophosphate (OP) poisoning.

OP poisoning is a major cause of death in the developing world, where organophosphates are used as pesticides (Buckley *et al.* 2004). Organophosphates have also been used as chemical warfare agents, although prohibited by the Geneva gas protocol, and in terrorist attacks (Solberg and Belkin 1997).

OP irreversibly inhibit the enzyme acetylcholine esterase (AChE), and causes extracellular accumulation of ACh. This, in turn, leads to excess stimulation of mAChR and nAChR (Taylor 1995). The mechanisms for seizures induced by OP poisoning include both cholinergic and glutamatergic effects (Solberg and Belkin 1997). None of the current treatment of OP poisoning include known blockers of the nAChRs (Sheridan *et al.* 2005).

A number of clinically used anti-cholinergic Parkinson drugs have been shown to be effective against OP-induced brain seizures (Shih *et al.* 1999). Notably, procylidine, biperiden and trihexphenidyl are mAChR antagonists and are also antagonists at NMDA-receptors (NMDA-R). The effects of these drugs at nAChR have not yet been determined.

Gacyclindine is a novel NMDA-R blocker with high affinity and apparently less neurotoxicity than other NMDA-R blockers (Hirbec *et al.* 2001a). Gacylidine is a phencyclidine (PCP)-derivate and is neuroprotective in animal models of excitotoxicity. The presence of at least one additional binding site distinct from NMDA-R has been established in rat brain and was implicated in the mechanism giving reduced neurotoxicity (Hirbec *et al.* 2001c, 2001b). The authors did not succeed in identifying this additional binding site.

HI-6 is an oxime used against OP poisoning. Oxime acts by reactivating action at on AChE. In addition, HI-6 was shown to give protective effects against OP poisoning when AChE was irreversibly inhibited and this effect was attributed to the block of muscle nAChR (Tattersall 1993). To further investigate this protective effect several non-oxime analogues of HI-6 have been synthesised, and their inhibitory effects on muscle nAChR have been studied (Timperley *et al.* 2005). The effect of these on the CNS and ganglia is not known and the compounds have not been tested on neuronal nAChR.

No cell line natively expresses the adult muscle nAChR, and therefore muscle tissue preparations are widely used as models for muscle nAChR block. No similar model tissue exists for receptors in the CNS, although primary cultures of dissected hippocampal neurons have been used. Recently, however, a human neuroblastoma cell line, SH-SY5Y, was used to study responses for neuronal nAChR (Dajas-Bailador *et al.* 2002).

The goal of this thesis was to develop a method for screening the effects of drugs on the neuronal nAChR. We then intended to use this method to screen relevant drugs for their possible action at nAChR, and if any were found, to characterise and quantify the inhibition.

1.2 Cellular calcium metabolism and signalling

The divalent cation Ca^{2+} regulates many activities in different cells, e.g. muscle contraction, carbohydrate metabolism, secretion, fertilization, neuronal excitability, cell growth, secretion, mitogenesis, and apotosis (Berridge and Bootman 1996; Alberts *et al.* 2002; Bird and Putney 2006). The changes in Ca^{2+} concentrations in the cytosol are subject to strict regulation, and are described in further detail below.

1.2.1 Plasma membrane Ca^{2+}-channels

There are three main types of Ca^{2+} channels in the plasma membrane; voltage operated Ca^{2+} channels, ligand-gated ion-channels, and store operated Ca^{2+}-channels.

Many different ligand-gated ion channels exist in the CNS and they are activated by the binding of agonists like glutamate, ACh or ATP. Most are mainly permeable to Na^{+}, and exert their effect by the depolarisation of the cell membrane (Alberts *et al.* 2002). A few ligand-gated ion channels have a significant permeability to Ca^{2+} as well; among the most notable in the CNS are the NMDA-receptor (NMDA-R) (Hassel and Dingledine 2006) and the nicotinic α7 homomeric receptor (Jensen *et al.* 2005; Hassel and Dingledine 2006). Neither receptor is selectively permeable to Ca^{2+}, but both show significant permeability to Na^{+} as well, and may therefore give both a Ca^{2+}-rise in the cells and a depolarisation of the cell membrane.

Voltage operated Ca^{2+}-channels (VOCC) open in response to depolarisation of the plasma membrane and allow extracellular Ca^{2+} to enter the cell (Berridge and Bootman 1996). They are found in a variety of excitable cells including neurons, myocytes and endocrine cells (Bird and Putney 2006). There are at least five different types of VOCC, differing in their gating kinetics, conductance and mode of inactivation. A main distinguishing feature is the depolarisation required to activate the channels. In particular L-type VOCC require a large depolarisation to open and are frequently activated as a consequence of depolarisation, giving rise to a large and sustained Ca^{2+}-influx (Dunlap *et al.* 1995; Berridge and Bootman 1996).

Store-operated Ca^{2+}-channels regulate what is known as capacitive calcium entrance. They respond do the depletion of intracellular stores, mainly in the endoplasmatic

reticulum (ER). They are mainly found in non-excitable cells, but also in some excitable cells (Parekh and Putney 2005; Bird and Putney 2006).

1.2.2 Ca^{2+} release from intracellular Ca^{2+}-stores

The main intracellular Ca^{2+}-stores in neuronal cells are the endoplasmatic reticulum (ER) and the mitochondria.

Ca^{2+} accumulates in the ER through the sarco/endoplasmatic reticulum Ca^{2+} ATPase (SERCA). SERCA uses the chemical energy of ATP to transport Ca^{2+} against its large electrochemical gradient from the cytosol to the ER. The ER releases Ca^{2+} to the cytosol and is involved in the Ca^{2+}-signalling through two distinct types of receptor; the IP_3-receptor and the ryanodine receptor.

Inositol 1,4,5 trisphosphate (IP_3) is a second messenger that releases Ca^{2+} from the ER via intracellular receptors. It is produced in the plasma membrane by cleavage of inositol containing phospholipids by PI phospholipase C. The cleavage is usually induced by the activation of certain G-protein coupled receptors, among them some muscarinic acetylcholine receptors (M_1, M_3, M_5) (Heacock and Fisher 2006). Binding of IP_3 to its receptor opens a Ca^{2+}-channel and results in increased cytosolic Ca^{2+}. Activation of IP_3 receptor channels is the main pathway to increased Ca^{2+} in non-excitable cells. It is also important in many neuronal cells, in response to neurotransmitters that work through G-protein coupled receptors (in particular those that work through the $G_{\alpha q}$-subunit) (Berridge and Bootman 1996; Bird and Putney 2006). Ca^{2+} is a positive allosteric modulator of the IP_3 receptor, giving calcium induced calcium release (CICR) from the ER, although IP_3 is required for channel opening (Berridge 1998).

CICR is normally associated with the ryanodine receptor. The ryanodine receptor is so named because of its strong affinity to the plant alkaloid ryanodine. The receptor opens in response to increased cytosolic Ca^{2+}, either from extracellular sources or from activation of IP_3-receptors. This process represent an internal amplification of the Ca^{2+}-signal, and its importance may vary in different cells (Berridge 1998; Bird and Putney 2006). In the neuroblastoma cell line SH-SY5Y, for example,

approximately 40% of the Ca^{2+} released by nicotine is released by secondary activation of the ryanodine receptors (Dajas-Bailador *et al.* 2002).

1.2.3 Mechanisms of Ca^{2+}-responses in the cell

Ca^{2+} may bind to - and regulate the activity of - several proteins in the cell. The best described of these proteins is calmodulin (CAM), which is found in all eukaryotic cells. The binding of Ca^{2+} to CAM induces a conformational change in CAM which imparts signalling information to a number of different molecules. Ca^{2+}-CAM activates a number of kinases, including general CAM kinases and more specialised kinases like myosin light chain kinase and elongation factor kinase. Calcineurin is a CAM-dependent protein phosphatase that plays an important role in the activation of lymphocytes and is the target of the clinically used immunosuppressant drugs ciclosporin and tacrolimus. CAM also regulates the secretion of Ca^{2+} by activation of the plasmalemmal membrane Ca^{2+} ATPase (PMCA). CAM also regulates formation of other second messengers including cyclic AMP (cAMP), nitric oxide (NO) and IP_3. A variety of cytoskeletal proteins, including tau and neuromodulin, are also regulated by CAM (reviewed in Berridge and Bootman 1996; Rang *et al.* 2003; Bird and Putney 2006).

Some effects are not mediated by CAM, but instead by direct effects of Ca^{2+} on target proteins. Most notable are the effects on Ca^{2+} on the secretion of neurotransmitters and contraction of skeletal muscle. In neurons, vesicles with neurotransmitter are docked at plasma membrane, but do not secrete their contents until a local rise in Ca^{2+} activates certain proteins and induces fusion of the vesicle to the plasma membrane and exocytosis (Alberts *et al.* 2002). In skeletal muscle the binding of Ca^{2+} to the protein troponin leads to disinhibition of myosin ATPase and the contraction of the muscle (Bird and Putney 2006).

Ca^{2+} is the key factor in the process of neurodegeneration known as excitotoxicity. Excitotoxicity is the mechanism where excessive stimulation of the neuron by glutamate causes cell death. It is an important mechanism for cell death implicated in a variety of different diseases and conditions, including Parkinson's disease, Alzheimer's disease, ischemic brain damage, motor neuron diseases, and OP poisoning (Solberg and Belkin 1997; Rang *et al.* 2003; Shaw 2005). The main

neurotransmitter behind this toxicity is glutamate. Excessive activation of different glutamate receptors results in increased cytosolic Ca^{2+}, which may result in increased production of reactive oxygen species (ROS) and NO, mitochondrial dysfunction, plasma membrane damage, and eventually apoptosis and necrosis (Rang *et al.* 2003).

1.2.4 Control of the cytosolic Ca^{2+}-concentration

For Ca^{2+} to work as an intracellular messenger, cells must maintain a low level of Ca^{2+} compared to the surroundings. Compared to the extra cellular levels of Ca^{2+} (~10^{-3} M), the intracellular concentration of Ca^{2+} is very low, 10^{-8}-10^{-7} M (Silver and Erecinska 1990).

Several mechanisms exist to restore the cytosolic Ca^{2+}-level after signalling. The most important are the Na^{+}/Ca^{2+}-exchanger, the plasmalemmal membrane Ca^{2+}-ATPase (PMCA), the sarco/endoplasmatic reticulum Ca^{2+} ATPase (SERCA), and the mitochondrial uptake. The Na^{+}/Ca^{2+}-exchanger is found in the plasma membrane and uses the electrochemical gradient for Na^{+} to extrude Ca^{2+} from the cell. The PMCA uses the energy of ATP to transport Ca^{2+} over the plasma membrane against the large electrochemical gradient. SERCA uses the chemical energy of ATP to transport Ca^{2+} against its large electrochemical gradient from the cytosol to the ER. Unlike the ER, mitochondria do not have a specific Ca^{2+}-transporter, but accumulates Ca^{2+} through an electrogenic Ca^{2+}-channel. The energy for driving Ca^{2+} into the mitochondria comes from the large negative membrane potential of the mitochondria. Under resting conditions the driving force is not large enough to give a significant increased influx of Ca^{2+} to the mitochondria. Once the threshold is reached, however, the driving force for uptake of Ca^{2+} is substantial. The mitochondrial transporter affinity is low, but the capacity is high and it is therefore important under conditions of high intracellular load. The transporter capacity of SERCA is much lower, but the affinity is high, giving the "final" adjustment to low intracellular levels of Ca^{2+} (reviewed in Berridge and Bootman 1996; Bird and Putney 2006).

1.3 Acetylcholine receptors

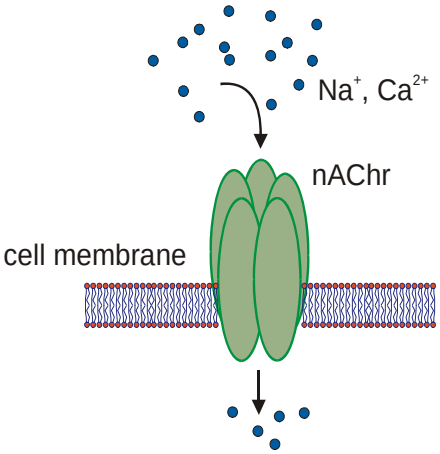

Figure 1-1 Nicotinic acetylcholine receptor. The five subunits form a pore through the cell membrane which allows the passage of Na^+ and sometimes Ca^{2+} into the cell.

Acetylcholine (ACh) exerts its effects on the central nervous system (CNS) through two distinct classes of receptors; the muscarinic and nicotinic actylcholine receptors (mAChRs and nAChRs, respectively). The mAChRs belong to the superfamily of G-protein coupled receptors. The mAChRs are coupled either to Ca^{2+}-raise, using inositol (1,4,5) trisphosohate (IP_3) as a second messenger (subtypes M_1, M_3, and M_5), or to inhibition of production of cAMP (subtypes M_2 and M_4) (reviewed in Taylor and Brown 2006).

Nicotinic acetylcholine receptors (figure 1-1) have three distinct functions. One type is found in muscle, where they invoke the end-plate potential and cause the contraction. Another type is found in the autonomic ganglia, and are exerting the control neurotransmission of the autonomic nerve system (Vander *et al.* 2001). In the CNS several types of receptors exist, their functions are outlined below. The nicotinic acetylcholine receptor is a ligand-gated ion channel. This means that a chemical signal binds to the receptor and opens the channel to ion flux. It belongs to the family of pentameric receptors that also include the $GABA_A$, glycine and 5-HT_3-receptors (Olsen and Betz 2006). These receptors constitute both the ligand-binding site and ionic pore through which the ions can flow when stabilized in the open configuration (Bertrand 2005). nAChRs consist of five subunits arranged around the central pore of the receptor (Brisson and Unwin 1984). The receptors in the CNS have similar composition, and vary mainly in their location relating to the blood brain barrier.

1.3.1 Neuronal nicotinic acetylcholine receptors

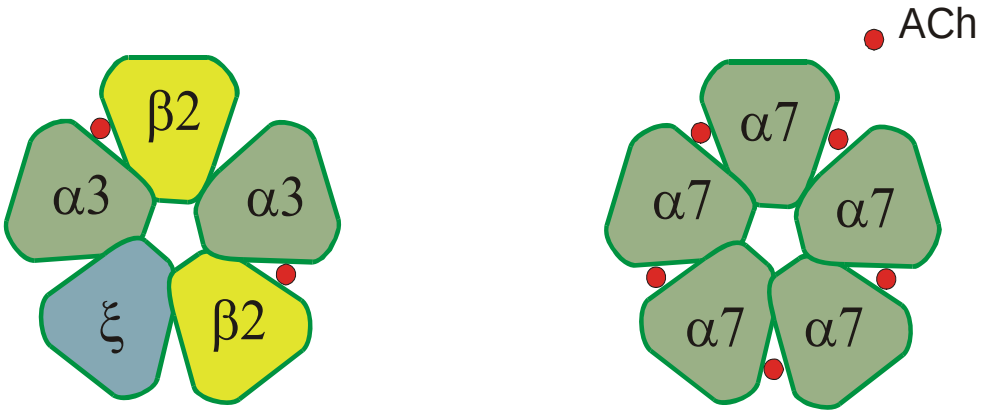

Figure 1-2 Top view of neuronal nicotinic receptors. A hetropentameric (left) and a homopentameric (right) receptor is shown. The binding sites for acetylcholine is shown in red. The ζ represents a subunit the can be of different types, and do not participate in the ligand binding.

For the neuronal nicotinic acetylcholine receptors (figure 1-2) the subunits are encoded by nine α (α2-α10) and three β (β2-β4) subunit genes, which are expressed in the nervous system and in non-nervous tissue (Gotti *et al.* 2006a). The α1 and β1 sununit are expressed in muscle. There are two main groups of neuronal nAChRs; the hetropentameric nAChRs usually consist of two α-subunits from the α2-α6-subunits, and three β-subunits, while the homopentameric nAChRs are usually formed from α7 or α9-subunits. The homopentameric nAChRs usually show a faster rate of desensitisation and a higher Ca^{2+}-permability than the heteropentameric nAChRs (Jensen *et al.* 2005).

Anatomical and functional evidence suggest that the nAChRs are located at both pre- and postsynaptic sites. At presynaptic terminals different subtypes regulate the secretion of neurotransmitters in different parts of the brain (Gotti *et al.* 2006b). Subtype localization is specific, and different subtypes may have opposing functions. This is consistent with the multitude of functions of nAChRs seen by the diverging effects of nicotine on behaviour (Picciotto 2003).

In rats, the heteromeric nAChRs have been implicated in the release of ACh, dopamine, noradrenalin and GABA, while the homomeric nAChs (mainly α7) was implicated in the release of GABA and glutamate (Jensen *et al.* 2005). nAChRs also appear to play a role in the development of the CNS (Gotti and Clementi 2004). In addition to its presynaptic role, nAChRs are also expressed at postsynaptic sites in the CNS. The precise role of these receptors has not yet been well defined, they seem to mediate fast effects on synaptic transmission and have long-term effects on gene expression and metabolic pathways. Presently, the presynaptic nAChRs have received the greatest attention and is believed to be of more critical physiological importance (Jensen *et al.* 2005).

Several effects of nAChRs in the brain and ganglia are known. *In vitro* experiments indicate that neuronal nAChRs (in particular α7) may control the development of neuronal architecture, stabilise synapse formation, and orient and control neurite outgrowth selection by means of various mechanisms, some of which may involve Ca^{2+}-influx (Gotti *et al.* 2006b). nAChRs are neuroprotective in several models of neuronal death. The intracellular steps that mediate this neuroprotective effect is not yet fully understood, but the effect is Ca^{2+}-dependent and does not involve block of glutamate receptor function. Thus, activation of downstream signalling pathways appears to be necessary for the prevention of neuronal death, but there is no consensus as to which pathway is the most important (Dajas-Bailador and Wonnacott 2004).

nAChRs have been implicated in diseases of the brain. Modifications in the number of nAChRs are seen in many different diseases, among these diseases are schizophrenia, Tourette's syndrome, attention deficient hyperactivity disorder, autism, depression and anxiety, and the neurodegenerative disorders Alzheimer's and Parkinson's diseases (AD and PD, respectively). Changes in nAChR expression is also seen in aging (Gotti *et al.* 2006a).

The early evidence for the involvement of nAChRs in AD and PD came from epidemiological data negatively correlating tobacco smoking with AD and PD. Careful studies confirmed the protective effect on tobacco smoking against PD, but failed to confirm the protective effect against AD. The pathology responsible for PD is the loss of dopaminergic function in the nigro-striatal pathway. There is also a dramatic decrease in functioning of the nicotinic cholinergic system that may be responsible for the deficit in the dopaminergic pathway and cortical function. Nicotine and nicotinic agents have been tested successfully in experimental models of PD, but clinical trials with nicotine have given controversial results; some improvement in cognitive and motor effects, but also an increase in tremor. In AD there is a decrease in the number of brain nAChR, particularly of the heteropentameric receptors. In AD nicotine improves perceptual and visual deficits, attention performance and semantic memory. Several drugs used against AD have effects on the nAChRs, among them memantine and the cholinesterase inhibitors tacrine and galantamine . Clinical trials of drugs with effects on nAChRs have so far been disappointing (reviewed in Gotti *et al.* 2006b).

1.4 Organophosphate poisoning

Organophosphates (OP) are a class of highly toxic compounds that includes nerve agents, pesticides and insecticides. Although the use of nerve agents is banned by the Geneva gas protocol, they were still used by Iraqi forces in the 1980s. Sarin, an OP nerve agent, was also used in the 1995 terrorist attack in the Tokyo subway (Solberg and Belkin 1997).

The main effect of OP is irreversible inhibition of AChE which results in inhibition of the hydrolysis of ACh and the excessive extracellular accumulation of ACh (van Helden and Bueters 1999; Sheridan *et al.* 2005). The main symptoms of OP poisoning are all related to the excessive stimulation of the cholingergic receptors: airway hypersecretion, bronchoconstriction, bradycardia, gut hypermotility, sweating and papillary constriction are all linked to mAChRs, while muscle fasciculation and weakness, tachycardia, hypertension, papillary dilatation, and irregular respiration are linked to nAChRs, both neuronal, ganglionic and muscular (Sheridan *et al.* 2005; Hassel 2006). CNS symptoms are also observed, among them giddiness, insomnia, tension, anxiety, central respiratory depression, ataxia, seizures, and coma (Barthold and Schier 2005). The cholinergic input to various brain nuclei gives rise to increased glutamatergic and GABAergic activity and causes brain seizures. The seizures progress rapidly to *status epilepicus*, which may lead to profound structural brain damage. The seizures and resulting brain damage are initiated by cholinergic over-stimulation which triggers seizures in susceptible brain regions. Once the seizures have started, non-cholinergic cell systems are progressively recruited and the seizures become resistant to muscarinic receptor antagonists. The seizures cause the release of excessive amounts of glutamate from affected neurons and the released glutamate give rise to excitotoxicity and cell death (Solberg and Belkin 1997).

1.4.1 Current treatment of organophosphate poisoning

The standard treatment for nerve-agent (OP) poisoning currently has two main parts. The treatment after exposure usually is atropine sulphate and one of the oximes obidoxime, P2S, 2-PAM, HI-6 or TMB4, injected intramuscularly. In some countries, including Norway, Great Britain and the United States, a benzodiazepine is added to this therapy. Atropine is an antagonist of the mAChRs, and blocks the over-activity of the mAChRs caused by organophosphate poisoning. The oximes reactivate AChE and reduce the problem of cholinergic over-stimulation. However, after some time, an irreversible change occurs in the binding of OP to AChE, and oximes no longer effectively reactivate AChE. Benzodiazepines are known anti-seizures drugs, and will reduce or stop the seizures observed in OP poisoning. Prophylactic treatment is used by the military when the risk of exposure is considered high. Currently, the reversible AChE inhibitor pyridostigmin, taken orally, is used by most countries (review in Aas 2003).

1.4.2 The role of nAChRs in organophosphate poisoning

The current treatment regimens for OP poisoning do not treat the nicotinic effects of OP poisoning. OP poisoning gives increased stimulation at all three locations of nAChR; the neuromuscular junction, the autonomic ganglia, and the CNS. At the neuromuscular junction OP poisoning results first in muscle fasciculation and then weakness or even paralysis (Barthold and Schier 2005). The weakness is probably due to desensitisation of the receptor (Sheridan *et al.* 2005). At the ganglia the excessive stimulation causes activation of the autonomic nervous system. While the activation of the parasympathetic nervous system is inhibited by the use of atropine, no drug in the treatment of the activation of the sympathetic nervous is commonly used, and tachycardia and hypertension usually result (Sheridan *et al.* 2005). The effects of OP poisoning on nAChRs have been difficult to assess. Some authors found no effects on survival after OP poisoning by the centrally acting nAChR antagonist mecamylamine *in vivo* (Shih *et al.* 1999), or on seizure activity in an hippocampal model of seizures (Harrison *et al.* 2004). However, a recent study using very high doses of mecamylamine did find an improvement in survival in mice. The main symptoms alleviated by mecamylamine were irregular respiration and convulsive crawling. It was suggested that these effects in the brain stem and that the effect of mecamylamine on OP poisoning was related to its effect in these areas of the brain (Hassel 2006).

1.5 Adenosin Trisphosphate as a neurotransmitter

Adenosine triphosphate (ATP) is the major form of energy in all living organisms. Somewhat surprisingly it is also an important neurotransmitter in the human body. There are two distinct classes of ATP-receptors, P2X-receptors, which are ligand gated ion-channels and P2Y-receptors, which are G-protein coupled receptors. Most P2Y-receptors in the CNS use IP_3 as a second messenger, and thus give an increase in intracellular Ca^{2+}. Some P2Y-receptors couple to a decrease in cAMP. Most P2X-receptors have a fairly large permeability to Ca^{2+}. ATP is usually co-released with glutamate, ACh or noradrenalin in the CNS. The main effects of P2X-receptors in the brain are in the release of glutamate in the hippocampus (reviewed in Burnstock 2006; Linden and Rosin 2006).

1.5.1 Purinergic receptors in astrocytes

Astrocytes express $P2Y_1$, $P2Y_2$, $P2Y_4$ and $P2X_7$ (Nedergaard *et al.* 2003). All the P_{2Y} receptors are linked to the generation of IP_3 and subsequent increase in cytosolic Ca^{2+} (Burnstock 2006). As noted above, $P2X_7$ is a ligand gated ion channel. $P2X_7$ have recently been implicated in induction of apoptosis (Runden-Pran *et al.* 2005). Astrocytes may therefore be used as a simple model of ATP responses in the CNS.

1.6 SHSY-5Y – A human neuroblastoma cell line

The human cell line SK-N-SH was isolated fra a bone marrow metastasis in a four year old girl (Biedler *et al.* 1973). The SK-N-SH cell line contains at least two different morphologicaly distinct cell types, one epithelial and one neuroblastoma. The cell line SH-SY5Y was cloned from its parent cell line SK-N-SH (Ross *et al.* 1983) and is neuroblast-like in appearance, with small to medium length neurites that extend radially from the cell body (figure 1-3). SH-SY5Y expresses both muscarinic acetylcholine receptors (mainly of the M_3 type) (Lambert *et al.* 1989) and several subtypes of nAChRs (Lukas *et al.* 1993). SH-SY5Y cells express the subunits α3, α5, α7, β2 and β4 (Lukas *et al.* 1993; Peng *et al.* 1994). The main functional types of nAChRs in SH-SY5Y are thought to be α3β2 and α7. (Dajas-Bailador *et al.* 2002). As SH-SY5Y expresses several of the nAChRs normally found in the CNS, it is a useful model of nicotinic receptors in the CNS (Peng *et al.* 1997; Dajas-Bailador *et al.* 2002; Sokolova *et al.* 2005).

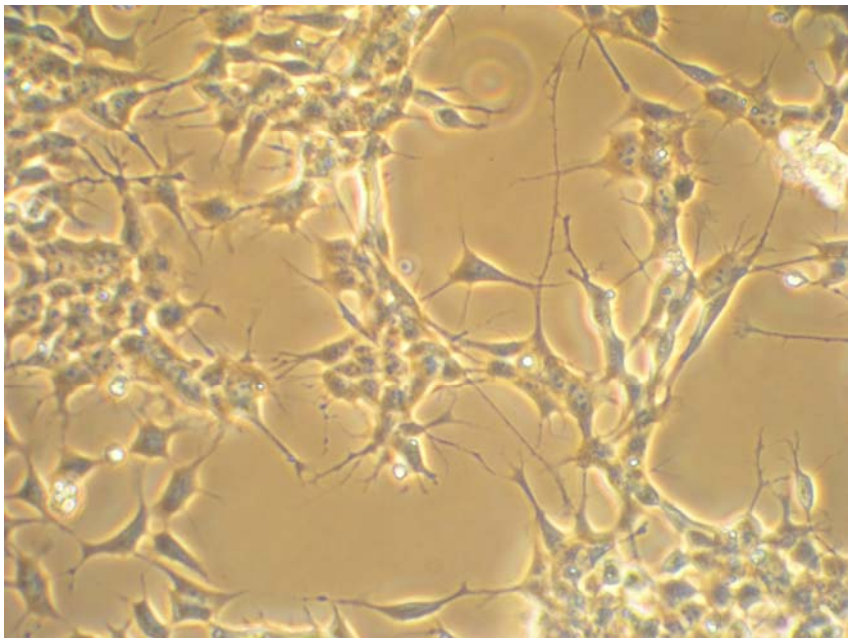

Figure 1-3 Phase-contrast photomicrograph of SH-SY5Y cells, passage 20, grown for three days on poly-D-lysine treated glass coverslips for single cell imaging. The cells shown are not confluent.

1.7 The different drugs investigated

1.7.1 Anti-cholinergic Parkinson drugs

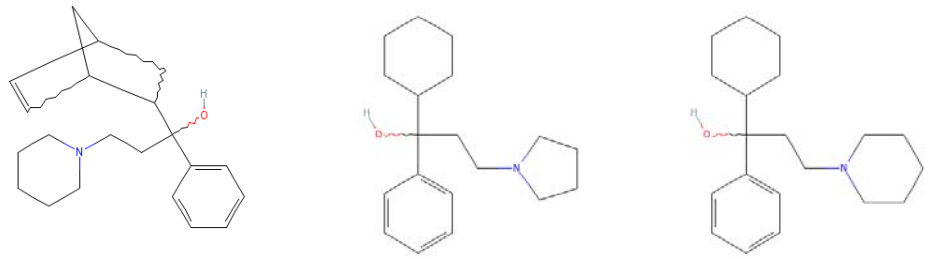

Figure 1-4 Anti-cholinergic Parkinson drugs: (left to right) biperiden, procyclidine and trihexphenidyl

The anti-cholinergic Parkinson drugs (figure 1-4) are the oldest form of anti-Parkinson drugs. After the introduction of L-DOPA and other dopamine agonists, however, they are not considered as first choice in the treatment of PD. They are now mainly used to treat extra-pyramidal side effects of antipsychotic drugs (Aasly 2004). They are also used to treat PD patients that can not use dopamine receptor-agonist and are sometimes used as an adjunct to L-DOPA therapy (Standaert and Young 1995). They have also successfully been used in treatment of dystonia and spasm. They are effective against soman-induced seizures in rats both after 5 minutes and after 40 minutes. The most potent of these drugs 5 minutes after soman poisoning are biperiden (ED_{50}: 0.09 mg/kg) and trihexphenidyl (ED_{50}: 0.17 mg/kg), while procyclidine is significantly less potent (ED_{50}: 1.51 mg/kg) (McDonough and Shih 1993; Shih *et al.* 1999). This correlates fairly well with the drugs potencies at the mACh IC_{50} of 8.4 nM, 26 nM and 70 nM, respectively (Syvälahti *et al.* 1988). Trihexphenidyl is the most potent 40 minutes after soman poisoning (ED_{50}: 6.49 mg/kg), followed by procyclidine (ED_{50}:13,30 mg/kg) with biperiden (ED_{50}: 19,05 mg/kg) as the least potent. Atropine does not stop seizures 40 minutes after soman poisoning (McDonough and Shih 1993; Shih *et al.* 1999). It has been shown that the anti-cholinergic Parkinson drug inhibit the NMDA-R. Their IC_{50}-values for inhibition of NMDA-induced responses in cocultures of rat cerebellar granule cells with astrocytes are 48µM for biperiden, 3 µM for procyclidine and 50 µM for trihexphenidyl (Ring and Tansø, unpublished data). The fact that atropine is not effective after 40 minutes is attributed to the recruitment of non-cholinergic pathways,

where glutamatergic pathways are thought to be most important (Solberg and Belkin 1997). The fact that the correlation between the potencies of the drugs at the NMDA-receptor and their effectiveness at stopping seizures after 40 minute is poor, may come down to differences in the pharmacokinetics of the different drugs. Relatively few studies on pharmacokinetics have been done on these drugs. The apparent volume of distribution (V_d) for trihexphenidyl is unknown, while the V_d for procyclidine and biperiden is 1.0 L/kg and 24 L/kg, respectively (Brocks 1999). For biperiden the concentration of drug in the brain has been reported as 10 times higher than the concentration in blood (Yokogawa *et al.* 1992). No such data exists for procyclidine or trihexphenidyl.

The anti-cholinergic Parkinson drugs have also been tested on effects of nicotine induced seizures *in vivo*. All the anti-cholinergic Parkinson drugs were effective with ED_{50} values of 4.6 mg/kg for biperiden, 3.1 mg/kg for procyclidine and 3.3 mg/kg for trihexphenidyl. The mechanism of the inhibition was not determined (Gao *et al.* 1998).

1.7.2 Memantine

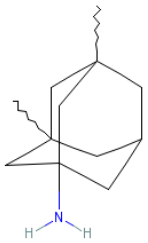

Figure 1-5 Memantine

Memantine (figure 1-5) is used clinically to treat moderate to severe AD at doses of up to 20 mg/day (Lundbeck A/S 2006). Clinically memantine shows significant positive effects on cognition, mood, behaviour and the ability to perform activities of daily living in patients suffering from moderate to severe AD (McShane *et al.* 2006). In humans a dose of 20 mg a day gives a blood serum concentration of 0.5-1 µM (Parsons *et al.* 1999) The unbound amount of drug in the cerebrospinal fluid is 40%-60% of the drug concentration in serum, giving clinically relevant brain concentrations of about 0.25-0.5 µM memantine (Kornhuber and Quack 1995). Memantine is classified as a non-competitive NMDA-R antagonist. Memantine has a reported IC_{50} of 1-3 µM in different systems. The inhibition of the NMDA-R is use-dependent and strongly voltage-dependent. Despite its relatively low affinity, memantine seems to bind selectively to the binding site of (+)-MK-801 (Parsons *et al.* 1999). Several different values have been reported for the IC_{50}-values of memantine on nAChR. Memantine blocks the α7-receptors with an IC_{50} of between 0.3 µM in hippocampal neurons (Aracava *et al.* 2005) and 5 µM in oocyte systems (Maskell *et al.* 2003). It blocks the α4β2-receptors with an IC_{50} of 7 µM in a stably transfected cell line (Buisson and Bertrand 1998). All of these effects were shown to be use-dependent. In addition to the effects on NMDA-R and nAChR, memantine also blocks voltage-operated Ca^{2+}-channels with an IC_{50} of 62 µM (Parsons *et al.* 1999). Memantine alleviates the convulsions caused by of OP poisoning, but does not stop seizures as monitored by EEG (Shih *et al.* 1999).

1.7.3 MK-801 and Gacyclidine

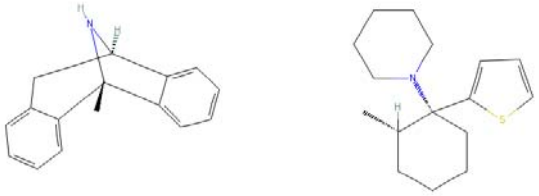

Figure 1-6 (+)-MK-801(left) and (-)-gacyclidine

(+)-MK-801(dizoclopine, figure 1-6) is a pharmacological tool often used to identify NMDA-R and NMDA-R dependent processes (Price *et al.* 1988; Briggs and McKenna 1996). It blocks NMDA-R in a voltage dependent manner and has its binding site in the ion channel of the receptor (Wong *et al.* 1986; Foster and Wong 1987; Price *et al.* 1988). MK-801 blocks the NMDA-R with an affinity of less than 100 nM (Wong *et al.* 1986) It blocks the α4β2 nAChR with an IC_{50} of 18.7 μM (Buisson and Bertrand 1998) and the α7 with an IC_{50} of 15 μM (Briggs and McKenna 1996). It is not used clinically because of intolerable side effects (Lipton and Rosenberg 1994).

Gacyclidine (GK11) is a novel antagonist of the NMDA-R that binds to the same binding site as MK-801. It has been shown to protect against glutamate neurotoxicity (Drian *et al.* 1999). Its (-) isomer has an IC_{50} of 2.5 nM at the NMDA-R, while its (+) - isomer has 10 fold lower potency (Lallement *et al.* 1997). The (-) isomer is more potent than the (+) in protection of glutamate induced toxicity, but no significant difference was found between the (-) isomer and the racemate (Drian *et al.* 1999). Gacyclidine is currently in clinical trials for treatment of acute traumatic brain injury (Lepeintre *et al.* 2004). It has been tested for acute spinal cord injury, but the results were disappointing (Fehlings and Baptiste 2005). It has also been shown to be neuroprotective against soman poisoning *in vivo* (Lallement *et al.* 1997; Bhagat *et al.* 2005). No data are currently available on the effect of gacyclidine on the nAChRs. Gacyclidine have, however, been shown to bind to a site distinct from the NMDA site in the brain of rats (Hirbec *et al.* 2001b).

1.7.4 Caramiphen

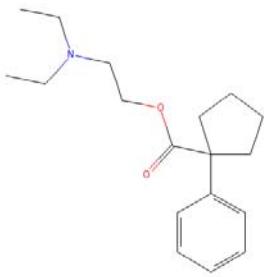

Figure 1-7 Caramiphen

Caramiphen (figure 1-7) is used clinically as an antitussive agent (Reisine and Pasternak 1995). It is an antagonist at both the mAChR and the NMDA-R. On the mAChR receptor it appears to be selective for the M_1 class of receptors with a K_i of 1,2 nM for M_1 and 32 nM at the M_2 mAChR (Hudkins *et al.* 1991). At the NMDA-R it has an IC_{50} in cocultures of rat cerebellar granule cells with astrocytes of 72 µM (Ring and Tansø, unpublished data). It is more protective against soman-induced seizures than the pure mAChR antagonist scopolamine when given as pre-treatment (Raveh *et al.* 2002). It protects both against soman-induced seizures and brain damage when given after exposure to soman, but does not stop seizures 40 minutes after soman exposure (Shih *et al.* 1999; Raveh *et al.* 2003). No studies of the effect of caramiphen on nAChR have been done *in vitro*, but caramiphen has an ED_{50} of 7.8 mg/kg against nicotine induced seizures *in vivo* (Gao *et al.* 1998), but the mechanism of this block was not clarified.

1.7.5 Novel bis-quarternary pyridine compounds

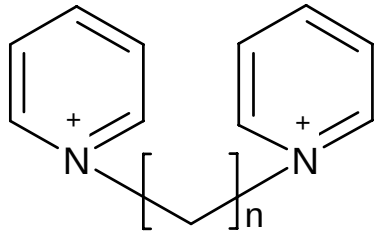

Figure 1-8 General structure of the novel bis-quarternary pyridine compounds tested. n is the chain length, varying from 1 to 10 for the compounds tested.

As noted above, the current treatment for OP poisoning does not affect nAChRs. However, HI-6, one of the oximes currently used to counter OP poisoning, does show an open-channel block of the muscular nicotinic ACh receptors (Tattersall 1993). As a result of this, the Defence Science and Technology Laboratories (DSTL) in Porton Down, UK, synthesised many analogues of HI-6 (figure 1-8) in order to test them on muscular nAChR (Timperley *et al.* 2005). These compounds are not oximes, but they were syntetized to be tested on muscle nAChR. Effects of the drugs on recovery of soman poisoned guinea pig diaphragm, a good model of muscle nAChR block, appears to be chain-length dependent with a bell-shaped response, where a chain-length of five gives the best response, while longer or shorter chain-lengths give less block. The effects on neuronal nAChR have not been determined.

1.8 Objectives

The objectives of this thesis were:

- To develop an effective and robust method for screening the effects of drugs at neuronal nicotinic acetylcholine receptors (nAChR).

- To use the method to test effects at neuronal nAChR by memantine, caramiphen, biperiden, trihexphenidyl and procyclidine. Of particular interest were NMDA-R inhibitors which show promise in the treatment of OP poisoning.

- To use the method to determine the effects at neuronal nAChRs by the novel neuroprotective agent gacyclidine, and to compare the effects of its racemate with its (-)-isomer.

- To compare the determined *in vitro* characteristics, with the available *in vivo* data in order to qualitatively asses the relevance of neuronal nAChR effects.

- To use the method to test for effects of several novel bis-quarternary pyridine compounds at neuronal nAChR and to compare these data with the data obtained *in vitro* at muscle nAChR by our collaborators at Porton Down.

.

2 MATERIALS AND METHODS

The main method used in this thesis is based on the measurement of intracellular calcium with the aid of fluorescent probes. The cells were loaded with exogenously added probes and the intracellular response was monitored by illumination with UV or visual light and then recording the fluorescent emission. Classical single cell imaging was used as well as a plate reader with cells grown in multi well plates.

2.1 Chemicals

Chemical name	*Supplier*
Akineton for injection 5 mg/ml (biperiden lactate)	Abbott, Fornebu, Norway
Adenosine triphophate, sodium salt	Sigma-Aldrich, St. Louis, MO
Atropine sulphate	Sigma-Aldrich, St. Louis, MO
Calcium chloride ($CaCl_2$)	Merck, Darmstadt, Germany
Caramiphen edisylate	Sigma-Aldrich, Milwaukee, WI
Carbachol	Sigma-Aldrich, St. Louis, MO
Deconex	Borer Chemie, Zuchwil, SUI
Dimethyl sulphoxide (sterile, water free)	Sigma-Aldrich, St. Louis, MO
EDTA, 0.02% in PBS	Sigma-Aldrich, St. Louis, MO
FLIPR Membrane potential assay kit	Molecular Devices, Sunnyvale,CA
Fluo-3-AM	Invitrogen, Paisly, UK
Foetal Bovine Serum	Invitrogen, Paisly, UK
Fura-2-AM	Invitrogen, Paisly, UK
(±)-Gacyclidine hydrochloride	Beufort Ipsen, Paris, France
(-) -Gacyclidine hydrochloride	Beufort Ipsen, Paris, France
Gentamycin sulphate	Sigma-Aldrich, St. Louis, MO
Glucose monohydrate	Merck, Darmstadt, Germany
GlutaMax®	Invitrogen, Paisly, UK
HI-6 diklorid monohydrat	Dr. Boulet, Defence Research Establishment Suffield, Ralston, Alberta, Canada
Horse Serum	Invitrogen, Paisly, UK

Hydrogen chloride (HCl) (Tritisol)	Merck, Darmstadt, Germany
Hydrogen peroxide (H_2O_2), 30%	Sigma-Aldrich, St. Louis, MO
Nicotine	Sigma-Aldrich, St. Louis, MO
Nicotine hydrogentartrate	Sigma-Aldrich, St. Louis, MO
Nitric acid (HNO_3), concentrated	VWR, Fountenay sous Bos, FRA
Magnesium sulphate heptahydrate ($MgSO_4 \cdot 7H_2O$)	Merck, Darmstadt, Germany
Memantine hydrochloride	Sigma-Aldrich, St. Louis, MO
Minimum Essential Medium (+Earle's –Glutamine)	VWR, Oslo, Norway
(+)-MK-801	Sigma-Aldrich, St. Louis, MO
Penicillin/streptomycin	Invitrogen, Paisly, UK
Pluronic F-127	Invitrogen, Paisly, UK
Poly-D-lysine (Molecular weight >300 000 D)	Sigma-Aldrich, St. Louis, MO
Potassium chloride (KCl)	Merck, Darmstadt, Germany
Probenecid	Sigma-Aldrich, St. Louis, MO
Procyclidine hydrochloride	Sigma-Aldrich, St. Louis, MO
Sodium chloride (NaCl)	Merck, Darmstadt, Germany
Sodium dihyrogenphosphate (NaH_2PO_4)	Merck, Darmstadt, Germany
Sodium hydroxide (NaOH)	Merck, Darmstadt, Germany
Sulphuric acid (H_2SO_4), concentrated	Merck, Darmstadt, Germany
Suramine	Sigma-Aldrich, St. Louis, MO
Trihexphenidyl hydrochloride	Sigma-Aldrich, St. Louis, MO
Trizma sulphate	Sigma-Aldrich, St. Louis, MO
(+)-tubocurarine hydrochloride hydrate	Sigma-Aldrich, St. Louis, MO
Verapamil hydrochloride	Sigma-Aldrich, St. Louis, MO

Unless otherwise stated all reagents were of *pro analysis* quality

2.2 Cell culture of SH-SY5Y

Culture medium for SH-SY5Y

0.1 mg/ml Gentamycin sulfate

10 % Foetal Bovine Serum

Minimum Essential Medium (+ Earle's + GlutaMax-I®)

SH-SY5Y (The European Collection of Cell Cultures, Salisbury, UK) was kept in ampoules at -135 °C in regular medium with the addition of 10% DMSO. The cells obtained at generation 14 were scaled up and stored at generation 17. The cells were removed from the freezer and left for 1 minute at room temperature before being heated to 37 °C in a water bath. The suspension of cells was added to 12 ml of medium and this suspension was added to a 75 ml flask (Sarstedt, Nürnbrecht, Germany). The cells were then incubated at 36 °C in an atmosphere saturated with water vapour and with 5 % CO_2 (Forma Scientific CO_2 water jacketed incubator, Forma Scientific inc., Ohio, USA). The medium was changed after one day to remove remnants of DMSO. The medium was changed after 3-4 days.

The cells were split every 6-8 days. The medium was removed and the cells were washed once with 2 ml 0.02% EDTA in PBS, this solution was removed, and 1.5 ml of EDTA was added. The cells were left for 2 minutes before the cells were detached with a light tap on the flask. 10 ml of medium was added to this suspension and transferred to a 15 ml tube (Sarstedt, Nürnbrecht, Germany). The suspension was then centrifuged for 3 minutes at 100 G (1000 rpm) (IEC centra CL 2, International Equipment Company, Tamro LAB, Vantaa, Finland).The supernatant was carefully removed, and the cells were resuspended in 5 ml of medium. For further culturing in flasks, 500 µl of cell suspension was added to 12 ml of medium, and this suspension was transferred to a new flask.

The cells were obtained mycoplasma free, and no further testing on the batches was performed as each batch was used for a limited period. There were no problems with fungal or bacterial growth in the incubator, which was dedicated to cell lines only. Experiments were run on cells from generation 19 to 25.

2.3 Measurement of intracellular Ca^{2+} and membrane potential

In general, an intracellular fluorescent probe reports changes of a concentration in a compartment of the cytoplasm. Visible or ultra violet (UV) light is used to excite the cell containing the probe, and fluorescent light that is then emitted by the probe is dependent on the concentration of the component it measures. For most probes, the binding of the component to be measured to the probe gives changes in the fluorescent properties of the probe. The best wavelength to excite the probe is determined by recording the excitation spectrum – varying the illumination wavelength, and determining which wavelength gives the highest emitted fluorescent intensity.

2.3.1 Fura-2, a ratiometric Ca^{2+}-probe

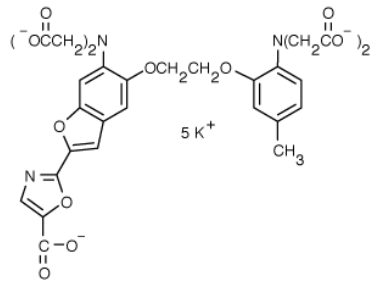

Figure 2-1 Fura-2 (pentapotassium salt)

Fura-2 (figure 2-1) is a ratiometric probe. A ratiometric probe does not simply change the emitted fluorescent intensity with changing concentrations of Ca^{2+}, but the Ca^{2+}-bound and Ca^{2+}-free probe has different spectra (figure 2-2). Because of this it is possible to excite at two different wavelengths and calculate the ratio of emitted fluorescence for the two intensities. (Grynkiewicz *et al.* 1985). Ratiometric measurements are largely independent of cell thickness, uneven probe loading, probe leakage and photo bleaching. For example, if probe leaks from the cells during the experiment, the intensity will be decreased, but as the calibration depends only on the ratio of intensities, the resulting ratio will not be affected (Tsien *et al.* 1985). To determine the ratio, the cells are excited with light alternating between two different wavelengths (340 nm and 380 nm), and the emission is measured at a fixed wavelength (510 nm).

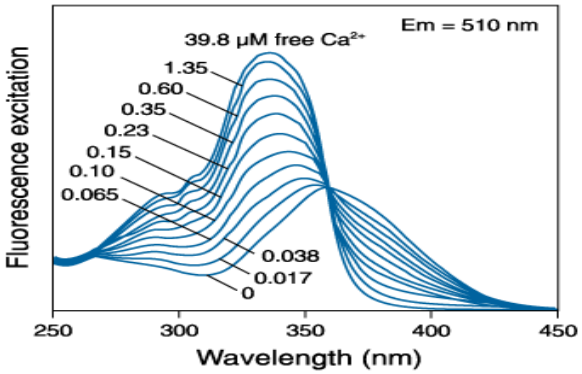

Figure 2-2 The excitation spectra of fura-2 at different wavelengths (from (Invitrogen 2006)

By first calibrating using the ratios obtained with solutions with known concentrations of Ca^{2+} and containing fura-2, it is possible to calculate the intracellular concentration of Ca^{2+} in any given experiment. If the ratio between the intensity at the two wavelengths is R, then the free Ca^{2+} have been shown to be

$[Ca^{2+}] = K_d(\frac{R - R_{\min}}{R_{\max} - R})(\frac{s_{f,2}}{s_{b,2}})$, where R_{min} is the limiting ratio when all the indicator is in the Ca^{2+}-free form (i.e. very low intracellular Ca^{2+}), R_{max} is the limiting ratio when probe is saturated with Ca^{2+}, K_d is the effective dissociation constant and $\frac{s_{f,2}}{s_{b,2}}$ is the ratio between the Ca^{2+}-free and the Ca^{2+}-bound form (Grynkiewicz *et al.* 1985; Kao 1994). Several factors may influence the K_d. Values ranging from 145 nM (*in vitro* without Mg^{2+}) to 373 nM (*in situ* in the astrocyte cell line U373-MG) have been reported (Grynkiewicz *et al.* 1985; Negulescu and Machen 1990; Petr and Wurster 1997). Fura-2 also shows some temperature dependence in its K_d (Oliver *et al.* 2000). The fluorescence at 380 nm becomes very small when Ca^{2+} is high, giving a large error in the ratio R_{max} because of uncertaincies in background corrections. Due to these and other uncertainties in calibrating Ca^{2+}-concentrations, responses are frequently reported as 340/380-ratio changes only and for the purposes of screening the relative potencies and determining IC_{50} and EC_{50} values this is adequate (Tsien and Harootunian 1990). The workload is significantly reduced by not calibrating in each experiments. The error in basal Ca^{2+}-levels has been estimated at 100 nM (Neher 1989), compared to a basal level of 10 – 100 nM (Silver and Erecinska 1990). Because of these problems the results of experiments with fura-2 will be reported as change in ratio, and not as change in intracellular Ca^{2+}-concentration.

2.3.2 Fluo-3, a single wavelength Ca^{2+}-probe

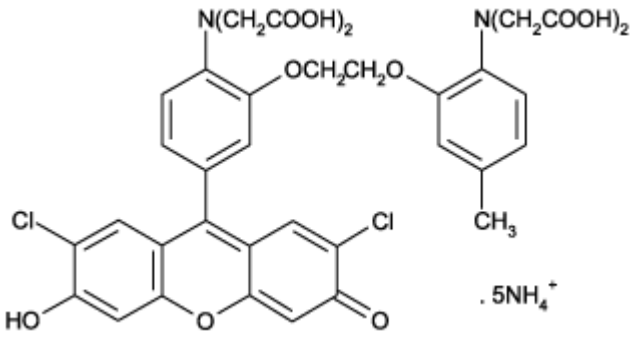

Figure 2-3 Fluo-3-AM (pentaammonium salt)

Fluo-3 (Figure 2-3) is a single wavelength probe. A single wavelength probe does not change its excitation or emission spectra as a response to various Ca^{2+} concentrations, but only changes the intensity of the emitted light. The Ca^{2+}-bound form of fluo-3 is 36-40 times brighter than Ca^{2+}-free probe (Minta *et al.* 1989). Unlike fura-2, fluo-3 is excited by visual light (485 nm), and has fewer problems with autofluorescence from cell components and the growth substrate. The results with fluo-3 are reported as changes in fluorescence. Typically fluo-3 is the probe of choice for qualitative measurements of fast changes in Ca^{2+}-concentration or when a high sensitivity for changes in Ca^{2+} is required. It is ideal for determining whether a drug blocks short "spikes" of Ca^{2+}-changes, e.g. from IP_3-mediated Ca^{2+}-release. It is used here to measure Ca^{2+}-responses of mAChRs as the responses to carbachol in SH-SY5Y is mainly due to IP_3-mediated Ca^{2+}-realease (Lambert *et al.* 1989; Taylor and Brown 2006).

2.3.3 The use of AM esters to load cells

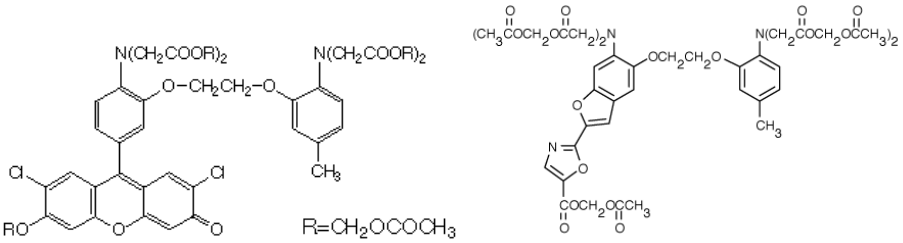

Figure 2-4 Fluo-3-AM and fura-2-AM

Both fluo-3 and fura-2 (figure 2-4) were used as their acetomethoxy (AM) esters. The AM group is used to mask the negative charges of these tetrecarboxylate probes. The uncharged and hydrophobic esters readily pass the lipid cell membrane and gain access to the interior of the cell. The carboxyl groups of the probes are important in sensing the Ca^{2+}; therefore, the AM group must be removed once the ester has entered the cell. The AM group is labile to enzymatic hydrolysis by intracellular esterases. This hydrolysis yields the tetracarboxylate form, which is effectively trapped inside the cells, resulting in an accumulation of the tetracarboxylate probe inside the cell (Tsien 1981; Kao 1994).

2.3.4 The membrane potential probe, FMP

The FLIPR Membrane Potential probe (FMP) is a novel fluorescent probe that responds to changes in membrane potential. Unlike the Ca^{2+}-probes, the FMP is not distributed to cytosol, but rather remains at the cell membrane. The FMP is much faster than traditional membrane potential probe $DiBAC_4(3)$, and its response-time is comparable to patch-clamp responses (Baxter *et al.* 2002). It is also the most sensitive fluorescent membrane potential probe currently available (Wolff *et al.* 2003). The probe was prepared in accordance with the recommended procedure; 1 vial was dissolved in 10 ml buffer. This solution was the frozen at -135 °C for later use.

2.4 Preparation of cell cultures in multiwell plates

A suitable method for screening should ideally have a number of characteristics: It should be quick, simple to use and robust against small variations in the experimental procedure. To be able to screen several drugs quickly a plate reader was used (BMG Fluostar Optima, BMG labtech, Offenburg, Germany). SH-SY5Y was chosen as the model system for central nicotinic effects. A method using fluo-3 has previously been described (Dajas-Bailador *et al.* 2002), but as the amount of fluo-3 used was rather high (10 μM) and fluo-3 is a single wavelength probe, it was decided to try to develop a more sensitive method using fura-2. As fura-2 is excited in the ultraviolet range, there is a considerable problem with autofluorescence, particularly from polystyrene based substrates. The requirements for a good growing substrate for this method is that it must have an acceptable (low) amount of autofluorescence at the wavelengths used and support the growth of the SH-SY5Y at sufficiently high density and thus give a good signal to noise ratio.

A number of different approaches were attempted as outlined below. The protocol that was accepted utilized a new, commercially available multiwell plate, Corning CellBind.

2.4.1 Treatment of polystyrene with ozone

Clear polystyrene sheets were cut to fit the measuring chamber (24x60mm). The slices were then treated with Daivonex to remove dust and impurities and were then rinsed with distilled water to remove remnants of the detergent. The slices were oxidised using UV-light/ozone (UVOCS, UVOCS, Montgomeryville, USA) for 10 minutes. The slices were then placed in a plate (NUNC, Roskilde, Denmark) with 4 rectangular wells, and 5 ml of 5 mg/ml sterile poly-D-lysine was added to each well. The slices were left in poly-D-lysine for 2-4 hours. While still in poly-D-lysine, the slices were sterilized for 20 minutes with UV-light. The slices were then washed with sterile water to remove the excess poly-D-lysine. Of the cell suspension gained from splitting the cells 1.6 ml was then diluted in 20 ml medium, and the resulting suspension divided evenly among the 4 wells. After three days, the cells were loaded with fura-2-AM as described below, using 5 ml medium for loading of cells with fura-2 for each slice. The slices were the fitted to a polycarbonate chamber with a stainless

steel bottom (Ring and Tansø, unpublished data) and experiments were run in the plate reader.

2.4.2 Treatment of polystyrene with a mixture of sulphuric acid and hydrogen peroxide

The polystyrene sheets were cut to fit the measuring chamber (24x60mm). Nine parts concentrated sulphuric acid and one part 30% hydrogen peroxide was mixed and allowed to cool before the slices were placed in this solution for 10-30 minutes. This mixture is extremely corrosive and may explode in contact with organic compounds, and requires extreme care when handling. The slices were then washed with distilled water and placed in a plate with 4 rectangular wells. The slices were then coated with poly-D-lysine and the cells plated as described above.

2.4.3 Treatment of glass coverslips with poly-D-lysine

Rectangular (24x60mm) glass coverslips (Menzel, Germany) were immersed in concentrated nitric acid over night and then washed in Daivonex for one hour in an ultrasound bath (Bransonic 5510, Bransonic Ultrasound Corp., Danbury, CT). The detergent was removed by washing with distilled water and the coverslips were placed in 96% ethanol. The ethanol was burned off and the coverslips were placed in a plate with 4 rectangular wells. The coverslips were then coated with poly-D-lysine and the cells plated as described above.

2.4.4 The commercially available plates: CellBind and Primaria

In addition to treating the surface, two commercially available 96-well plates were tested; Corning CellBind® (Corning, Corning, NY) and Primaria® (Lev). Primaria is the plate used in the previous study (Dajas-Bailador *et al.* 2002). Both plates were used without pre-treatment. Of cell suspension obtained from splitting the cells 1 ml was added to 12 ml of medium and this suspension was divided to the 96-wells (125 µl/well).

2.5 General procedure for experiments on the plate reader

2.5.1 Solutions

Medium for loading of cells with fura-2:

4 μM Fura-2-AM (4 mg/ml)

0.2 % Pluronic F-127

1 mM Probenecid

Culture medium for SH-SY5Y

Medium for loading of cells with fluo-3:

10 μM fluo-3-AM (11.5 mg/ml)

0.2 % Pluronic F-127

1 mM Probenecid

Culture medium for SH-SY5Y

Medium for deesterification:

1 mM Probenecid

Culture medium for SH-SY5Y

Experimental buffer:

140 mM NaCl

15 mM Tris-HCl

5 mM glucose

3.5 mM KCl

2 mM $CaCl_2$

1.2 mM Na_2HPO_4

1 mM $MgSO_4$

Double distilled water

This solution was bubbled with O_2. The solution used in the injectors was placed in an exsiccator for 5 minutes. This was done to avoid bubbles forming during the experiments as the injected volumes were small and applied via tubing connected to syringes.

2.5.2 The plate reader

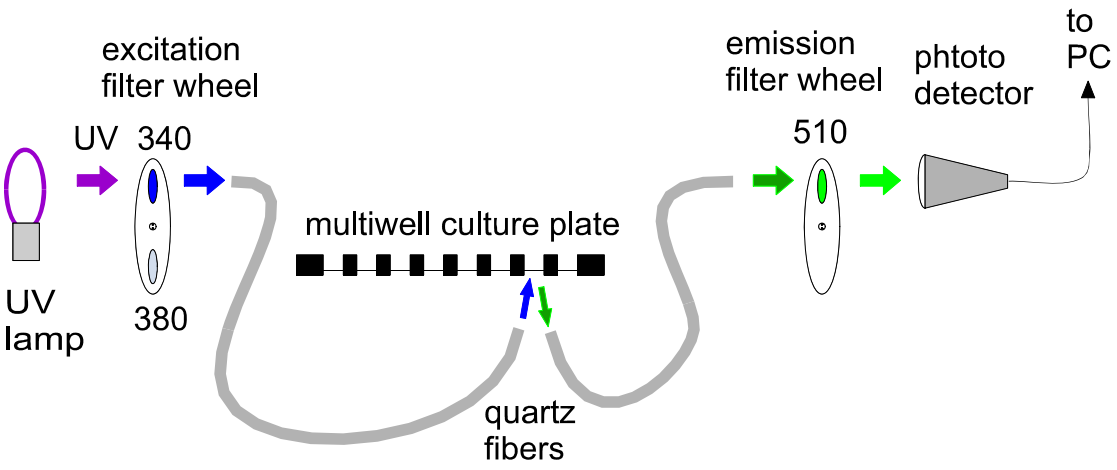

Figure 2-5 A sketch of the imaging part of the plate reader. The image shows the principle measurement with fura-2, but the same applies to other probes. The numbers refer to wavelength of the filters. UV: Ultra violet.

The BMG FluoStar Optima plate reader is controlled by a computer. It has to injectors that can be filled with experimental solutions; the temperature can also be set. Both the injectors and the lens are stationary, while the plate is moved around. Light is sent from an UV lamp through a excitation filter and a quartz fibre to the plate. The emitted light is sent through another quartz fibre to a filter, and then to a photo detector which sends an electrical signal to the computer for analysis. The filter wheel can switch between the filters to allow for ratiometric measurements (figure 2-5).

2.5.3 Experimental procedure

SH-SY5Y cells were cultured as previously described and the medium was changed to the medium for loading the cells with fura-2 or fluo-3, respectively. The detergent pluronic F-127 was used in the loading medium to increase the cellular uptake of the probe and the solubility of AM esters (Kao 1994). Probenecid was added, at 1 mM, as it inhibits the organic anion transporters and thus increases the amount of fura-2 or fluo-3 in the cytosol of the cells (Di Virgilio *et al.* 1990). For each well, 125 µl was used and the cells were placed in the incubator for 45-60 min. The medium for loading was then replaced with the medium for deesterification and put back in the incubator for 25-40 minutes. The plates were then removed from the incubator, and

the cells were washed once with experimental buffer before adding experimental buffer and antagonist to a total volume of 200 µl in each well. The agonist was diluted in experimental buffer and filled in the injector. The plate was then placed in the plate reader set at a temperature of 32 °C. The total measurement time for each well was 30 seconds and 9 seconds for fura-2 and fluo-3, respectively. The agonist was injected under the computerised control of the plate reader after 8 seconds (fura-2) or 3 seconds (fluo-3). The injection speed was 100µl/s, and the total injection volume was 50 µM, except for experiments with K^+-depolarization, where the injection volume was 100 µl.

2.6 Single cell imaging

Round glass coverslips with a diameter of 18 mm were treated as described above for rectangular coverslips and transferred to a 12-well plate (NUNC, Roskilde, Denmark). Cells were split as described above, and 1 ml of the resulting suspension was transferred to each well. The cells were grown for 2-4 days before experiments.

2.6.1 The imaging system

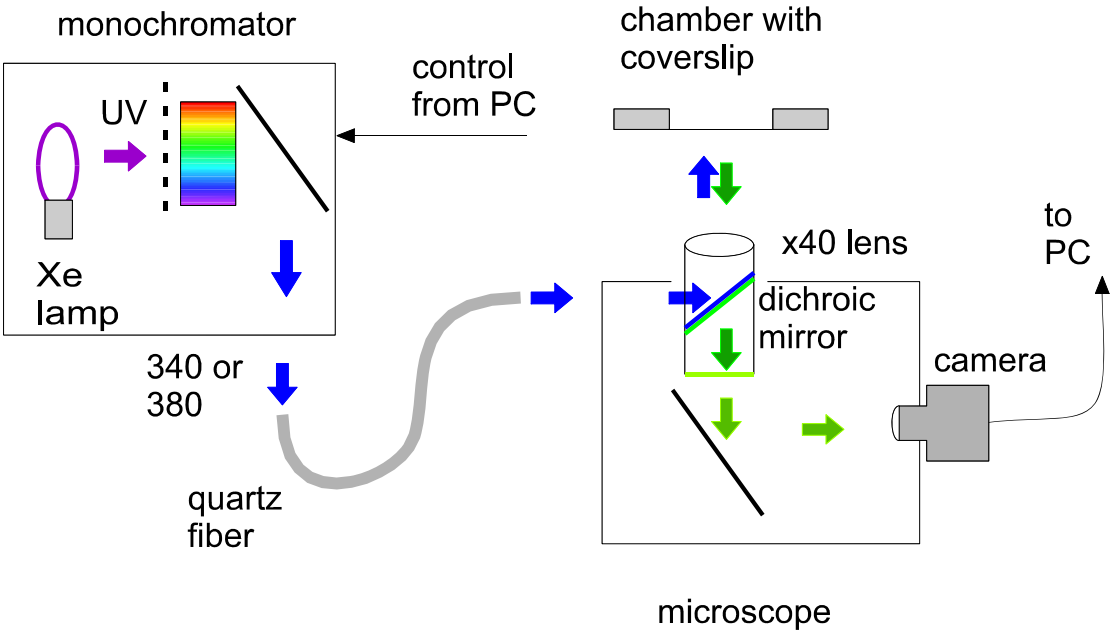

Figure 2-6 Sketch of the imaging system. The system used for fura-2 is shown, but the same applies for other probes. The numbers refer to wavelength. UV: Ultra violet.

The different components of the imaging system are shown in figure 2-6. The heart of the system is the microscope, Olympus IX70 (Olympus). The experiments were started so that the computer could control the monochromator (Polychrome II, TILL-Photonics). The monochromator has a UV-lamp with a mirror that was moved by a computer controlled motor, allowing the alteration of wavelengths between 340 nm and 380 nm for fura-2. The light is led to the microscope by a quartz optical fibre and was reflected onto the cells by a dichroic mirror (i.e. a mirror that reflects certain wavelengths, but not other wavelengths). The emitted light passes through the dichroic mirror, as its wavelength is longer, and then through a filter. The filtered light was detected with a CCD (charged coupled device) video camera (Imago, advanced cooled imaging, TILL-photonics) coupled to a computer.

2.6.2 Single cell imaging of Ca^{2+}-responses

All experiments were run using fura-2. While still in the wells, the medium was changed to medium for loading the cells with fura-2, and the plate was placed back in the incubator for 45-60 minutes. For each well 1 ml was used. The medium for loading was then replaced with the medium for deesterification and put back in the incubator for 20-50 minutes. The coverslip with the cells was removed from the plate and transferred to a chamber with a stainless steel bottom and upper part made of Teflon. The chamber was assembled using screws. An O-ring sealed the upper part to the coverslip. The same experimental buffer that was used in the experiments with the plate reader was used in these experiments. The cells were washed twice with the experimental buffer. The volume of experimental buffer was fixed at 500 µM. The chamber with cells was then placed on the microscope. The excitation wavelengths were 340 and 380 nm and the emission was measured at 510 nm. The drugs were applied using a pipette.

2.6.3 Single cell imaging using the membrane potential probe

The coverslip with the cells were removed from the plate and transferred to a chamber similar to the one used for measurements of Ca^{2+}, only smaller. This chamber was used to keep volumes small, as FMP is expensive. The same experimental buffer that was used for experiments with the plate reader was used for these experiments as well. The cells were washed twice with 100 µl of experimental buffer. 100 µl experimental buffer and 100 µl of the FMP solution was then added to the cells and the cells were left to equilibrate for 25-35 minutes. The chamber with cells was then placed on the microscope. The excitation wavelength was 500 nm and the emission was measured with a low pass filter with cut off at 540 nm (i.e. summing all emission with wavelength >540 nm). The drugs were applied to the cells using a pipette.

2.7 Astrocytes

2.7.1 Culturing astrocytes

Medium for astrocytes

Penicillin/Streptomycin (GIBCO)

15% Horse Serum

Minimum Essential Medium (+ Earle's + GlutaMax-I®)

Astrocytes were kept in ampoules at -135 °C in regular medium with the addition of 10% DMSO. The cells were previously prepared by dissection and culture from cerebella of 7 days old rat pups as previously described (Hertz *et al.* 1989). Primary cultures were grown for 21 days before being stored at -135 °C. The ampoules were removed from the freezer and left for 1 minute at room temperature before warming to 37 °C in a water bath. The content of each ampoule was then mixed with 12 ml medium, and the resulting suspension was plated out into a 96-well optical bottom plate (NUNC, Roskilde, Denmark). The cells were then incubated at 36 °C in an atmosphere saturated with water vapour and with 5 % CO_2. The medium was changed after one day to remove remnants of DMSO. The medium was changed every 3-4 days.

2.7.2 Experiments with astrocytes

The solutions used were the same as for SH-SY5Y. The astrocytes were cultured for 14-21 days before the experiments. The procedure used was as for SH-SY5Y except that the cells were loaded for 60 minutes and deesterified for 30 minutes.

2.8 Data analysis

Raw data from the plate reader were analysed by subtracting a pre-measured background from the raw data. The ratios were then calculated by dividing the intensity at 340 nm by that at 380 nm. For further analysis the average of the first 4 measurements were taken as the base line, and the average of the last 10 measurements were taken as the peak intensity. The 4-parameter logistic equation (Hill equation) was then fitted to the data using GraphPad Prism version 4.00 for Windows, (GraphPad Software, San Diego California USA, www.graphpad.com). The equation is: Y = Bottom + (Top-Bottom) / (1 + 10^ ((LogEC50-X)*HillSlope)), where X is the logarithm of concentration and Y is the response. All the concentrations were first transformed to the logarithms of the concentration. The Bottom value was fixed at 0. This equation corresponds to the Hill equation: $y = y_{\max} \frac{[A]^{n_H}}{IC_{50}{}^{n_H} + [A]^{n_H}}$ (Jenkinson 2002). In order to compare different data from different experiments, the data from these experiments were normalized prior to analysis as the maximal response varied between experiments. The resulting data were compared using the F test (Motulsky and Christopoulos 2003). A Hill coefficient (n_H or HillSlope) different from unity is an indication of receptor kinetics more complex than first order kinetics id the receptor is studied directly (Barlow and Blake 1989), however, in this thesis we measure down stream effects of receptor stimulation, and the Hill coefficient is taken simply as a parameter to get a good fit of the model. As the IC_{50} values obtained in this way have an asymmetrical confidence interval, the 95% confidence interval of the IC_{50} is quoted in stead of the Standard Error (SE) in the tables (Motulsky and Christopoulos 2003). The SE values are fairly small, so for convenience, the data will be shown as ± an average SE in the text. Average SE is taken as half the average difference between 95% confidence interval limits and the average. (i.e. $\frac{(IC_{50}(upper) - IC_{50}) + (IC_{50} - IC_{50}(lower)}{4}$, where IC_{50}(upper) and IC_{50}(lower) is the upper and lower limit of the 95 % confidence interval).

3 RESULTS

3.1 Single cell Ca^{2+}-imaging of SH-SY5Y

The initial objective was to establish a plate reader method to characterize the effects of drugs on responses to nicotine mediated by nAChR. The responses measured in a plate reader are the average of a large number of cells. In order to characterize the responses to nicotine and to determine the dynamics of the responses in single cells, single cell Ca^{2+}-imaging was first performed on SH-SY5Y. Experiments were also made to determine the effects of some antagonists, to establish whether Ca^{2+}-measurements could be used as an indicator of block of nAChR. A typical response to nicotine is shown below (figure 3-1). The response to nicotine shows a fast increase in $[Ca^{2+}]_i$ with a return to the base line within minutes. At 30 µM nicotine, the desensitation was significant and no sustained responses were possible. Larger doses gave faster desensitation, and a dose of 30-50 µM was judged as suitable for use with the plate reader. Single cell images of K^+-depolarisation are shown in figure 3-4.

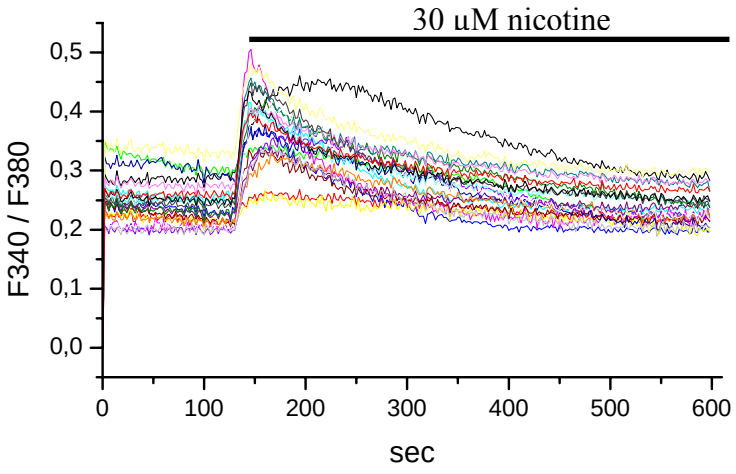

Figure 3-1 Typical response to 30 µM nicotine in SH-SY5Y. F340/F380 fluorescent emmision ratio, where a rise indicate increased $[Ca^{2+}]_i$. The response is a fast rise followed by return to the baseline, due to desensitisation of nAChR. Cells were grown for three days on glass coverslips, and incubated with fura-2 for 45 minutes prior to use. Nicotine was added using a pipette.
Each line is the ratio from a single cell.

To see the effects of one known and one potential antagonist, these were added before nicotine in the single cell imaging experiments. Typical graphs for 20 µM memantine (a known antagonist) and procyclidine (a possible antagonist) are shown below. Both completely blocked the nicotine-induced responses (figures 3-2 and 3-3).

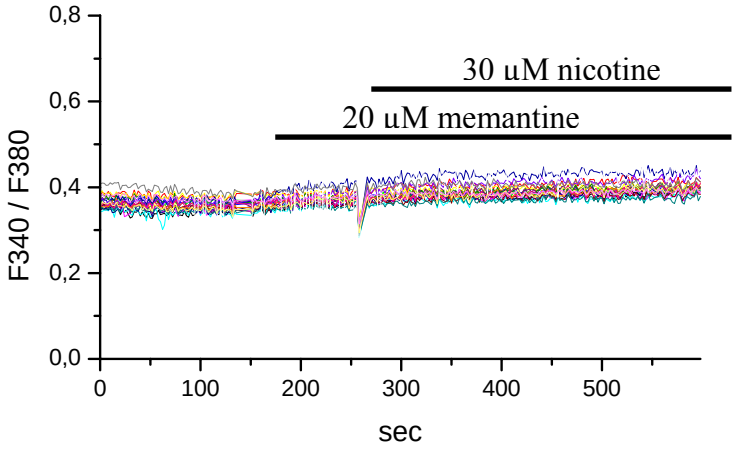

Figure 3-2 Inhibition of nicotine induced $[Ca^{2+}]_i$-increase by 20 µM memantine. Addition of nicotine has no effect on ratio. Cells were grown for three days on glass coverslips, and incubated with fura-2 for 45 minutes prior to use. Drugs added by pipette. F340/F380 is fluorescent emmision ratio, where a rise indicate increased $[Ca^{2+}]_i$.

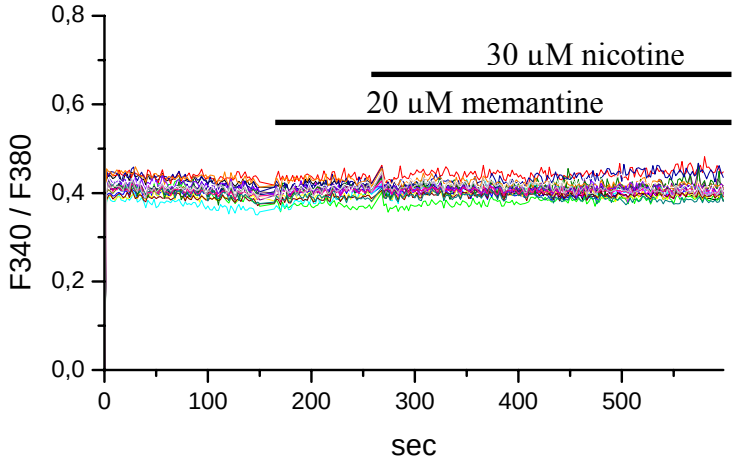

Figure 3-3 Inhibition of nicotine induced $[Ca^{2+}]_i$-increase by 20 µM procyclidine. Addition of nicotine has no effect on ratio. Cells were grown for three days on glass coverslips, and incubated with fura-2 for 45 minutes prior to use. Drugs added by pipette. F340/F380 is fluorescent emmision ratio, where a rise indicate increased $[Ca^{2+}]_i$.

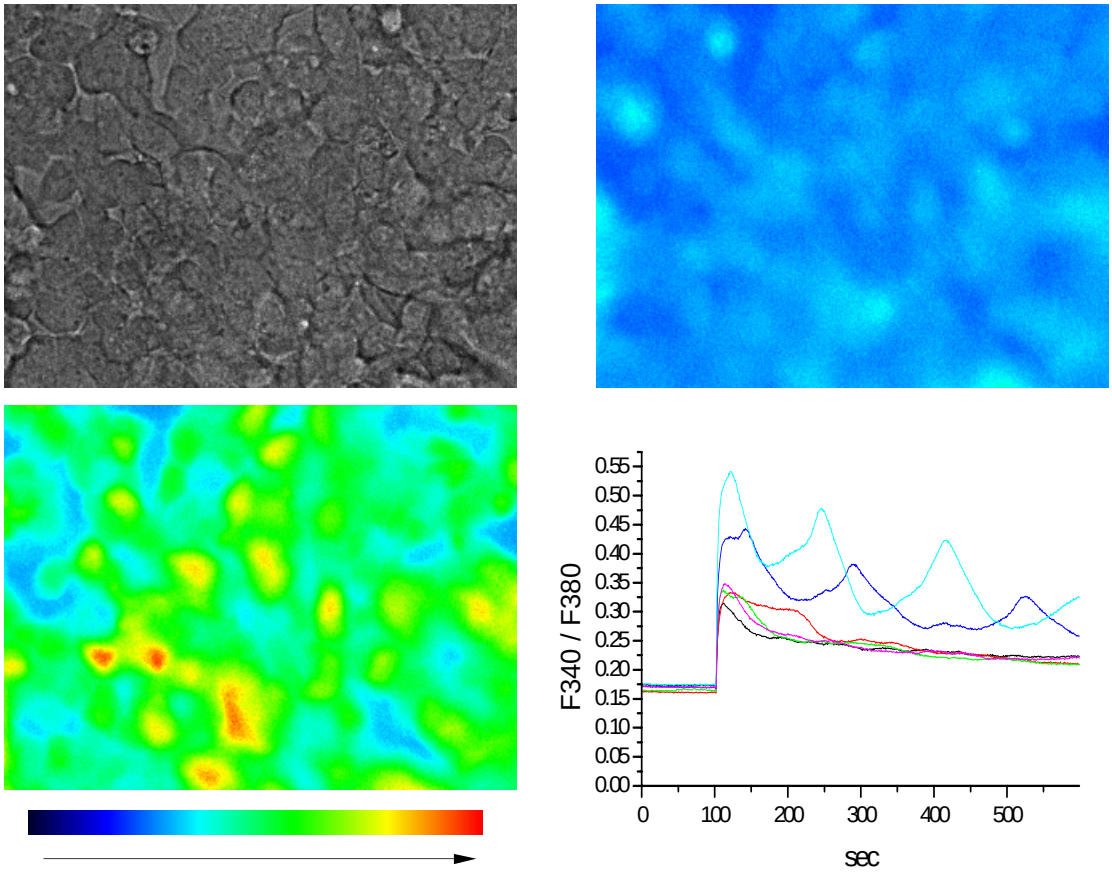

Figure 3-4 Ca^{2+}-response of confluent SH-SY5Y cells to stimulation by depolarisation 50 mM K^+. Transmission image (top left), fluorescence image before (top right) and after addition of 50 mM K^+ (bottom left). Single cells may be obscure in confluent cultures. Increasing F340/F380 from blue to red. For comparison the kinetic data from this experiment are shown at bottom right. F340/F380 is fluorescent emmision ratio, where a rise indicates increase in $[Ca^{2+}]_i$.

3.2 Development of the screening method

The initial experiments were aimed at developing a protocol for an efficient method with high signal to noise. As noted in the methods section, the choice of cell culture substrate is not trivial and a number of attempts were made in order to find a suitable substrate.

Both systems using polystyrene sheets (i.e. home made coverslips), the sheets were oxidised to enable coating with poly-D-lysine. The oxidisation, however, resulted in unacceptable high levels of autofluorescence. The glass coverslips have very low autofluorescence, but the SH-SY5Y cells did not grow well on this substrate, and the substrate was thus discarded for use in the plate reader. In contrast, glass coverslips can be used for single cell imaging, where measurements are made in single cells and no advantage is gained if the cell layer is confluent. In the plate reader, however, a high density of cells gives a better signal to background margin, and therefore a more reliable result. The Primaria plates also gave an unacceptable high level of autofluorescence when using 340 nm and 380 nm excitation with fura-2. The novel CellBind plates had both an acceptable low level of autofluorescence, and supported a confluent growth of SH-SY5Y. Thus CellBind plates were chosen for further experiments.

Using SH-SY5Y cells cultured on CellBind a dose-respose curve for nicotine was obtained (figure 3-5). The maximum response was obtained with 50 μM nicotine. At higher concentrations of nicotine the response was lower, probably as a result of the desensitization of the nAChRs. An EC_{50} of 16.8 μM ± 1.5 μM was obtained by best-fit of the Hill equation (see methods). In further experiments 50 μM nicotine was therefore used. Initially only 48 wells were run in each experiment, resulting in a total recording time of 25 minutes. Further testing and analysis found no difference in running 48 or 96 wells at a time in this system, even though the last well was run 50 minutes after the first. 96 wells were therefore run at a time as this increased the number of parallels. Typical responses from a single experiment are shown in figure 3-6.

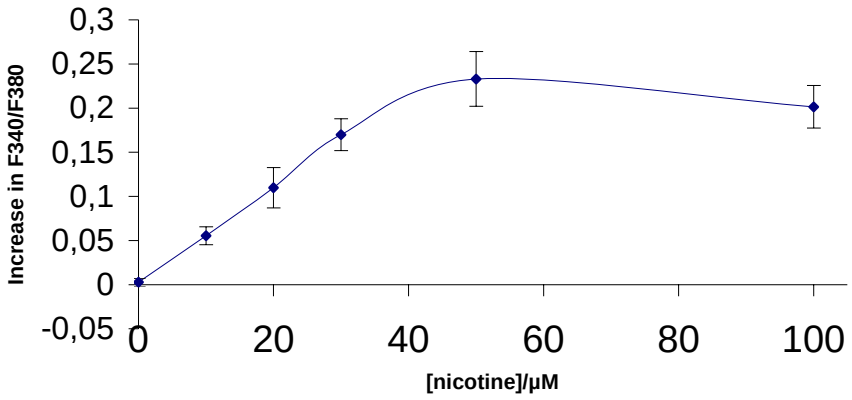

Figure 3-5 Dose-response curve for calcium responses of SH-SY5Y cells to nicotine.
Cells grown for three days on a CellBind multiwell plates and incubated with fura-2 for 45 minutes. Average Ca^{2+}-response ± SEM are shown at each concentration. F340/F380 is fluorescent emission ratio, where a rise indicate increased $[Ca^{2+}]_i$. n=8.

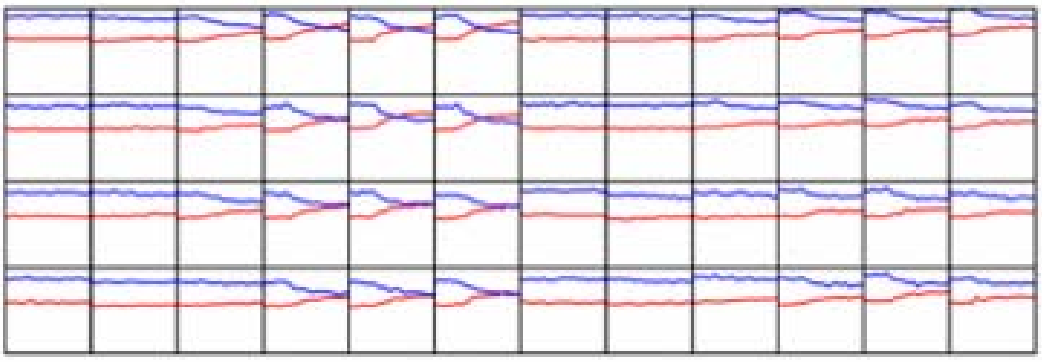

Figure 3-6a Typical "raw data" for single well responses for 48 of the 96 wells in a dose response experiment for calcium responses of SH-SY5Y cells to nicotine. Cells were grown for three days on a CellBind multiwell plate and incubated with fura-2 for 45 minutes. The red line is fluorescence for excitation at 340 nm (F340), the blue line at 380 nm (F380). The increase of F340 and decrease of F380 is a clear indication of intracellular Ca^{2+} rise. Columns 1-6 (from left) are dose-responses to nicotine alone, while columns 7-12 is a dose-response with 1 µM trihexphenidyl, an anticholinergic Parkinson drug, added. Doses were (left to right) 0 µM, 5 µM, 10 µM, 20 µM, 30 µM, and 50 µM. The same doses were used with trihexphenidyl in the bath.

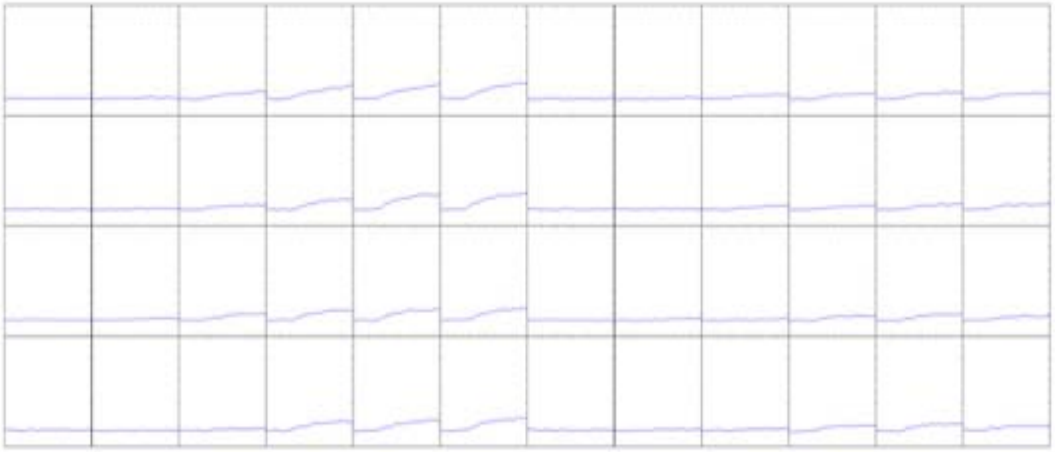

Figure3-6b Typical ratios for single well responses for 48 of the 96 wells in a dose response experiment for calcium responses of SH-SY5Y cells to nicotine. These are the ratios to that corresponds to the data of figure 3-6a. Cells were grown for three days on a CellBind multiwell plate and incubated with fura-2 for 45 minutes. Columns 1-6 (from left) are dose-responses to nicotine alone, while columns 7-12 is a dose-response with 1 µM trihexphenidyl, an anticholinergic Parkinson drug, added. Doses were (left to right) 0 µM, 5 µM, 10 µM, 20 µM, 30 µM, and 50 µM. The same doses were used with trihexphenidyl in the bath.

3.3 Determination of IC_{50} for inhibition of nicotine induced Ca^{2+}-responses in SH-SY5Y

3.3.1 Drugs that block the NMDA-receptor

Name	logIC_{50} ±SE	IC_{50}	95 % Confidence interval of IC_{50}	Hill coefficient ±SE
Biperiden	0.19 ± 0.03	1.56 µM	1.36 - 1.79 µM	-1.49 ± 0.13
Caramiphen	-0.49 ± 0.03	0.323 µM	0.287 - 0.363 µM	-1.22 ± 0.08
(±)-Gacyclidine	-0.53 ± 0.04	0.296 µM	0.247 - 0.355 µM	-1.51 ± 0.16
(-)-Gacyclidine	-0.78 ± 0.03	0.163 µM	0.139 - 0.190 µM	-1.34 ± 0.11
Memantine	0.45 ± 0.04	2.85 µM	2.37 - 3.41µM	-1.16 ± 0.12
(+)MK-801	0.25 ± 0.06	1.80 µM	1.40 - 2.31 µM	-1,31 ± 0.16
Procyclidine	0.14 ± 0.04	1.38 µM	1.14 - 1.66 µM	-1.41 ± 0.17
Trihexphenidyl	-0.13 ± 0.04	0.75 µM	0.627 - 0.895 µM	-1.34 ± 0.14

Table 3-1 IC_{50} values for block of nAChR-responses by different NMDA-R blockers. All values are obtained by best-fit of the Hill-equation as described in the methods section. Values are pooled data from at least two independent experiments. n=6-8.

SH-SY5Y cells were cultured for 3 days in CellBind plates, and the $[Ca^{2+}]_i$–responses were obtained using 50 µM nicotine. The logIC_{50}, IC_{50} and Hill coefficient values were obtained from best-fit of the Hill equation, as described in the data analysis, section from pooled data of at least two independent experiments for each drug.
The IC_{50} value was 1.56 µM ± 0.11 µM for biperiden, 0.323 µM ± 0.019 µM for caramiphen, 0.296 µM ± 0.027µM for racemic gacyclidine, 0.163 µM ± 0.013µM for (-)-gacycldine, 2.85 µM ± 0.28 µM for memantine, 1.80 µM ± 0.23µM for MK-801, 1.38 µM ± 0.13µM for procyclidine and 0.75 ± 0.07 µM for trihexphenidyl. For the anticholinergic Parkinson drugs, trihexphenidyl was significantly more potent than procyclidine and biperiden, while there was no significant difference between biperiden and trihexpenidyl. In experiments in a single plate, no significant difference was found between racemic and (-)-gacyclidine, although further studies indicate the (-)-gacyclidine may be slightly more potent. The results are shown in table 3-1 and inhibition curves are shown in figure 3-7.

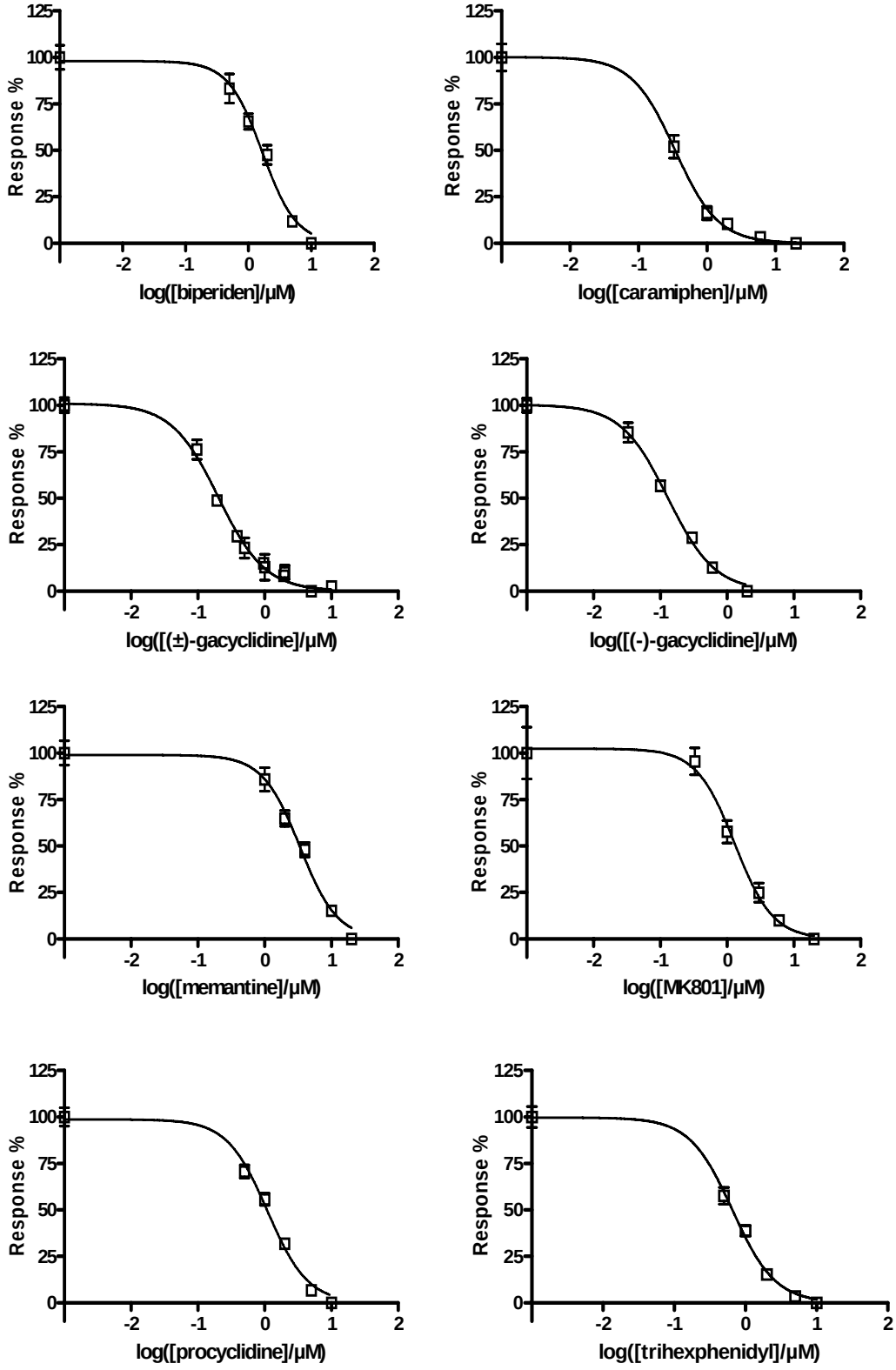

Figure 3-7 Best-fit curves for inhibition of nicotine induced Ca2+-responses in SH-SY5Y. Cells were grown for three days on CellBind multiwell plates and incubated with fura-2 for 45 minutes. Average Ca2+-response ± SEM are shown at each concentration. The response is shown in % of maximum response. n=6-8

3.3.2 Novel bis-quarternary pyridine compounds

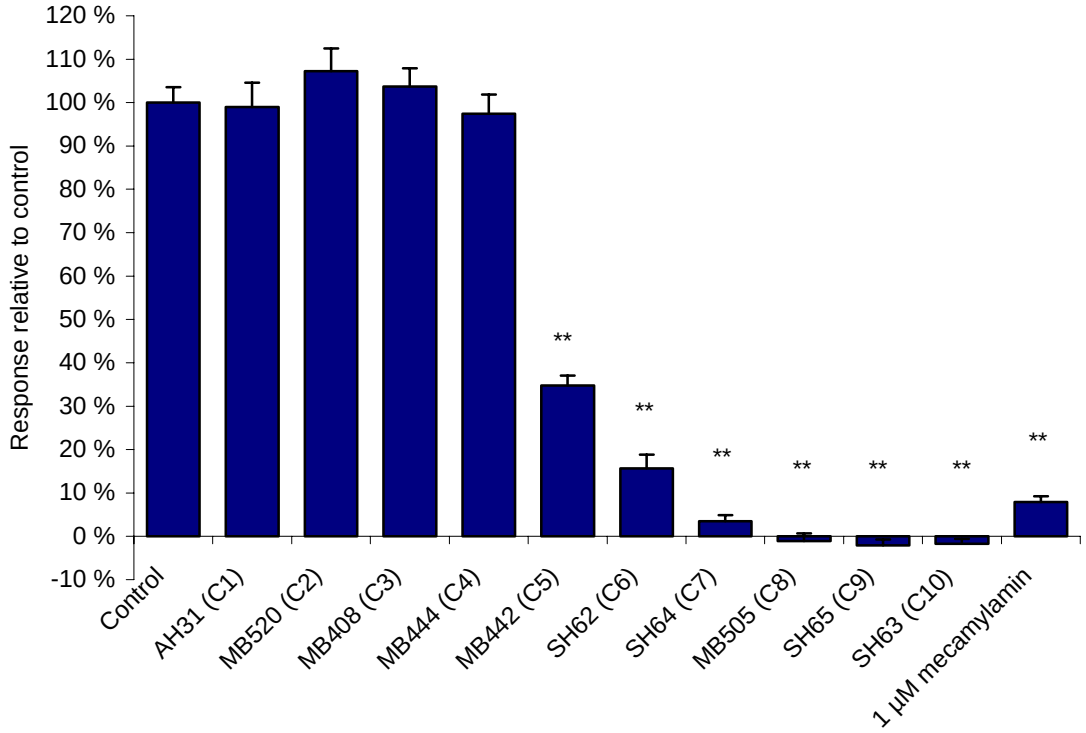

Figure 3-8 Inhibition of nicotine (50 µM) induced Ca2+-responses in the neuroblatoma cell line SH-SY5Y by novel bis-quarternary pyridine compounds. Cells were grown for 3 days on Cellbind multiwell plates and incubated with fura-2 for 45 minutes. All drugs were tested were at 100 µM. Mecamylamine is a known neuronal nAChR blocker and was used as positive control. Average Ca2+-response with SEM are shown for each drug. All responses were normalised to the response to nicotine without inhibitor (control) taken as 100%. n=8. ** p<0.01, ANOVA with Dunnett's *post hoc* test.

In an initial experiment all the compounds, with chain length from 1 to 10 carbon atoms, were tested at a high concentration to screen for blocking activity. SH-SY5Y cells were cultured for 3 days, and the Ca^{2+}–responses were obtained using 50 µM nicotine. The compounds with chain lengths C1-C3 did not show any inhibition of nAChR-responses (figure 3-8), and their IC_{50} values were therefore not determined. The $logIC_{50}$, IC_{50} and Hill coefficient values were obtained from the Hill equation as described in the data analysis section from pooled data of at least two independent experiments, except for MB444 where only data from a single experiment was used. The block decreases for increasing chain length, with an fairly linear relationship between the $logIC_{50}$ and the chain length. The IC_{50} values ranged form 439µM ± 49 µM for MB444 (C4) to 1.68 µM ±0.13 for SH63 (C10). The results for the blocking

action on neuronal nAChR are summarized in table 3-2. Inhibition curves for these compounds are shown in figure 3-9.

Name	Chainlength	logIC_{50} ±SE	IC_{50}	95 % Confidence interval of IC_{50}	Hill coefficient ±SE
MB444	C4	2.73±0.04	539 µM	447 - 650 µM	-1.81±0.26
MB442	C5	1.99±0.04	98.0 µM	82.1 - 116.9 µM	-2.1±0.4
SH62	C6	1.46±0.04	28.5 µM	24.3 - 33.5 µM	-1.88±0.24
SH64	C7	1.57±0.05	37.2 µM	30.0 - 46.1 µM	-1.8±0.3
MB505	C8	1.24±0.03	17.2 µM	14.8 - 20.2 µM	-1.74±0.22
SH65	C9	0.62±0.04	4.20 µM	3.56 - 4.96 µM	-1.66±0.20
SH63	C10	0.22±0.03	1.68 µM	1.44 - 1.95 µM	-1.28±0.09

Table 3-2 IC_{50} values for block of nAChR-responses by novel bis-quarternary pyridine compounds. All values are obtained by best-fit of the Hill-equation as described in the methods section. Values are pooled data from at least two independent experiments, except for MB444. n=6-8.

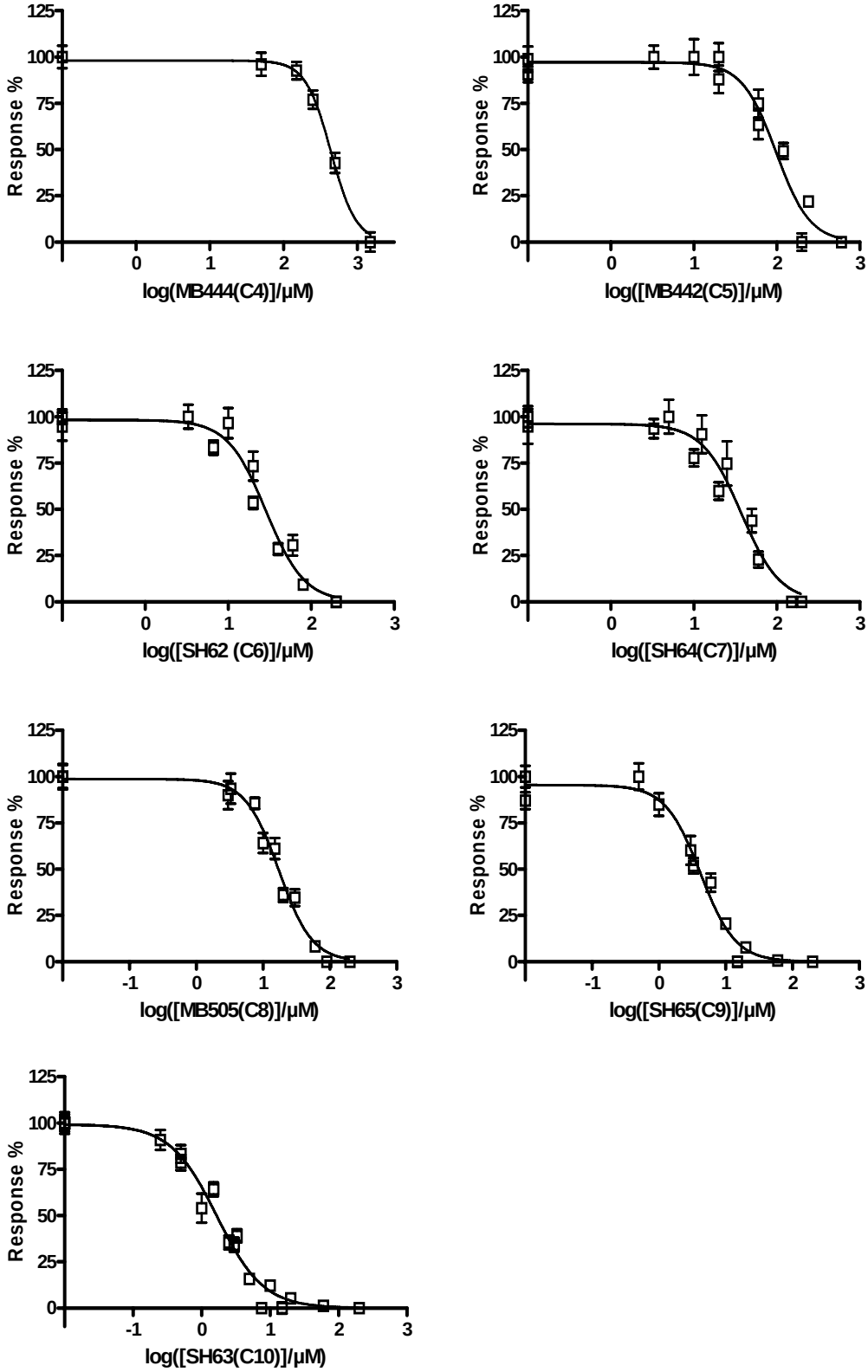

Figure 3-9 Best-fit curves for inhibition of nicotine induced Ca^{2+}-responses in SH-SY5Y. Cells were grown for three days on CellBind multiwell plates and incubated with fura-2 for 45 minutes. Average Ca^{2+}-response ± SEM are shown at each concentration. The response is shown in % of maximum response. Data from at least two experiment for all compounds except MB444 (C4). n=6-8.

3.4 Testing the use dependence of the block of the nicotine induced Ca^{2+}-responses by certain drugs

	IC_{50} at 25 µM nicotine ± average SE	IC_{50} at 250 µM nicotine ± average SE	Ratio of IC_{50}s (25µM/250µM)	p-value for difference
Biperiden	1.47 ±0.21 µM	0.66 ±0.10 µM	2.81	0.0002
(±)-gacyclidine	0.31 ±0.07 µM	0.16± 0.04 µM	1.82	0.059 n.s
(-)-gacyclidine	0.23 ±0.04 µM	0.083 ±0.011 µM	2.82	0.0001
Mecamylamine	0.025 ±0.007 µM	0.023 ±0.03 µM	1.1	0.76 n.s.
Memantine	3.2 ±0.9 µM	1.05 ±0.15 µM	3.05	0.0021
MK-801	2.4 ±0.3 µM	1.8 ±0.3 µM	1.33	0.31 n.s.
Procyclidine	1.6 ±0.4 µM	0.98 ±0.16 µM	1.70	0.083 n.s.
Trihexphenidyl	1.11 ±0.20 µM	0.50 ±0.05 µM	2.19	0.0002
SH63 (C10)	3.2 ±0.8 µM	1.7 ±0.3 µM	1.77	0.044
(+)-tubocurarine	0.66 ±0.16 µM	0.64 ±0.06 µM	1.03	0.92 n.s.

Table 3-1 IC_{50}-values of inhibitors of nAChR-responses in SH-SY5Y with 25 µM and 250 µM nicotine. Cells were grown for three days on CellBind multiwell plates and incubated with fura-2 for 45 minutes. Data were obtained by best-fit of the Hill equation as described in methods. All data shown ± average SE. P-values are from F tests. n.s.: not significant.

The manner of block is physiologically and clinically relevant. The use-dependence of an inhibitor is important since one wishes that the inhibition should be low for normal physiological conditions whereas the block should be significant for conditions of excess stimulation of nAChRs, such as is expected when the AChE is inhibited (e.g. in organophosphate poisoning). We were interested in testing whether the drugs showed a use dependence in their block of the nAChR, i.e. whether the degree of activation of the receptors influenced the value of the IC_{50}. In order to test this, the IC_{50} of the drugs were determined for two different concentrations of nicotine; 25 µM and 250 µM (table 3-3). These concentrations were chosen because both give measurable Ca^{2+}-responses to nicotine and are significantly different doses. SH-SY5Y cultured as described above for 3 days were loaded with fura-2 and experiments run as described above. If the IC_{50}-values were significantly ($p < 0.05$) smaller at 250 µM

than at 25 µM the result was taken as a indication of use-dependence. In brief, biperiden, (-)-gacyclidine, memantine, trihexphenidyl and SH63 (C10) showed signinficant use-dependence, while mecamylamine, MK-801, and (+)-tubocurarine did not. Procyclidine and racemic gacyclidine did not reach significance, but this may be due to insensitivity of the method. The graphs for SH63, procyclidine and (+)tubocurare are shown below (figure 3-10).

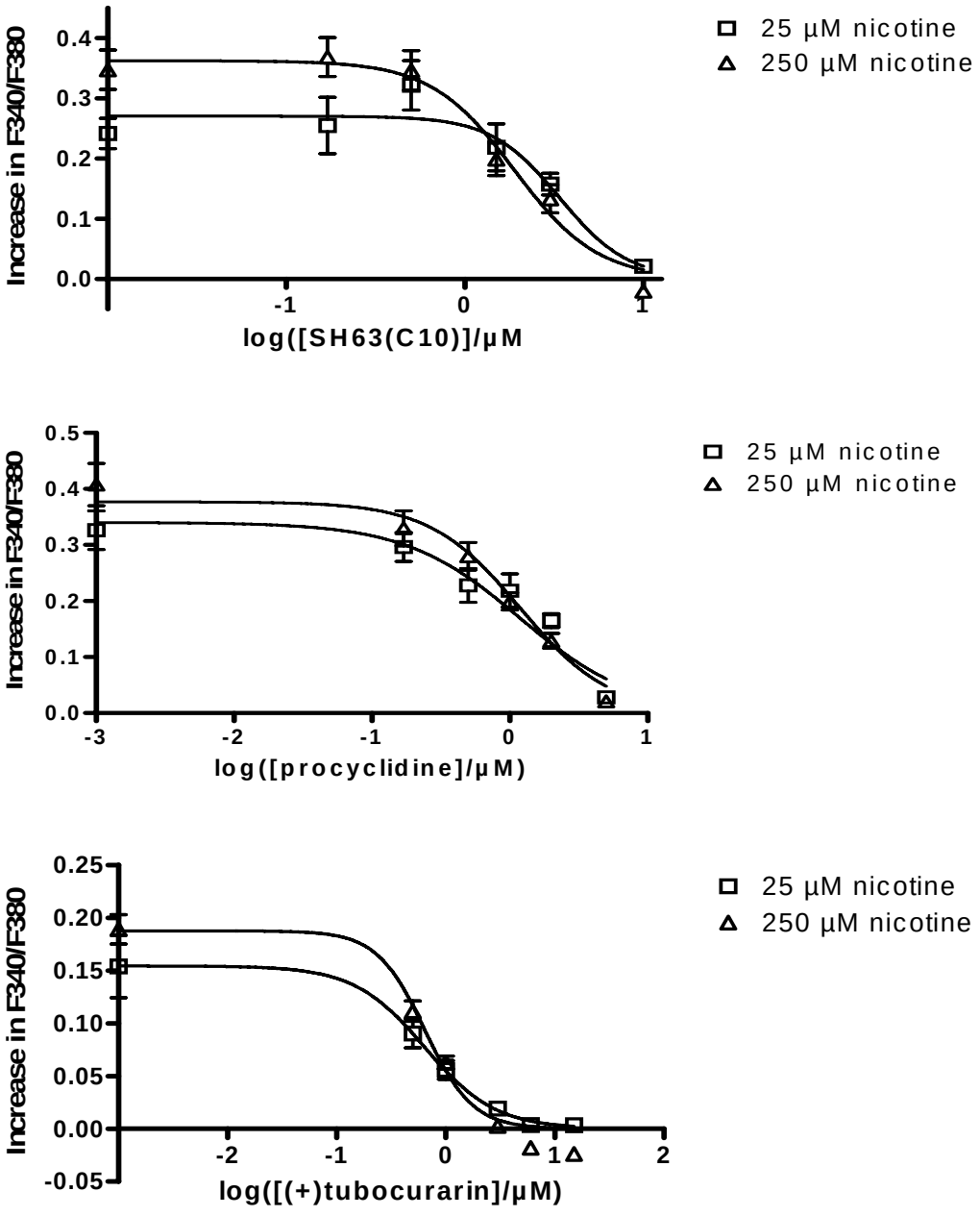

Figure 3-10 Inhibition curves with high (250 µM) and low (25 µM) nicotine for SH63, procyclidine and (+)-tubocurarine. F340/F380 is fluorescent emission ratio, where a rise indicate increased $[Ca^{2+}]_i$. Cells were grown for three days on CellBind multiwell plates and incubated with fura-2 for 45 minutes. Average Ca^{2+}-response ± SEM are shown at each concentration. n=8.

3.5 Voltage dependence of block of nAChR-responses

Similar to use dependence, the voltage dependence is of interest since one wants a greater degree of block when the neurons are depolarized, whereas there is no use for inhibition when the neurons are at the resting level. The voltage dependence of the block of nAChRs by procyclidine, memantine and MK-801 were tested by changing the concentration of K^+ in the experimental buffer to 2.5 mM (low membrane potential) and to 10 mM (high membrane potential) and then obtaining inhibition curves as described above. For procyclidine the IC_{50} values at low and high membrane potential were 1.26 ± 0.07 μM and 1.05 ±0 .06 μM, respectively. For memantine the IC_{50} values were 2.00 ± 0.21 μM and 1.35 ± 0.18 μM, respectively. The differences were significant for both procyclidine and memantine ($p < 0.037$). For MK-801 the IC_{50} values were 1.29 ± 0.11 μM and 1.07 ± 0.08 μM, respectively. This different was not significant ($p < 0.118$). There was no significant difference between the Hill slopes for either experiment. The inhibition curves for these experiments are shown in figure 3-11.

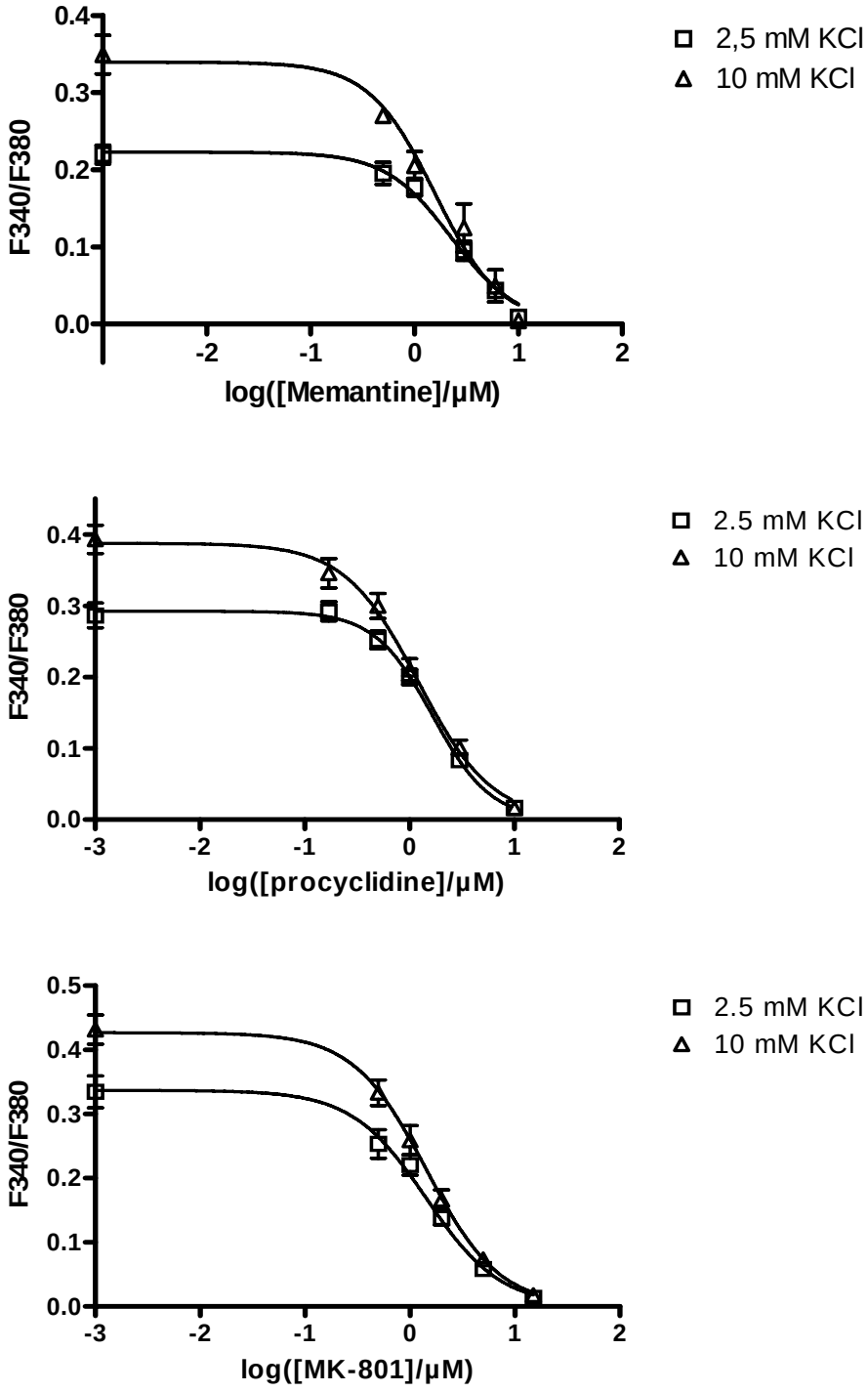

Figure 3-11 Inhibition curves with high (10 mM K^+) and low (2.5 mM K^+) for memantine, procyclidine and MK-801. F340/F380 is fluorescent emission ratio, where a rise indicate increased $[Ca^{2+}]_i$. Cells were grown for three days on CellBind multiwell plates and incubated with fura-2 for 45 minutes. Average $[Ca^{2+}]_i$ at each concentration shown ± SEM. n=6-8.

3.6 Screening of effects on voltage-operated Ca^{2+}-channels

All the drugs tested blocked nicotine induced Ca^{2+}-responses. A part of this block is expected to be due to direct block of influx through neuronal nAChR. Nevertheless, a significant part of the Ca^{2+}-response is a downstream effect due to influx through voltage operated Ca^{2+}-channels (VOCC), since depolarisation due to opening of the channels activates these channels (Dajas-Bailador *et al.* 2002). It was therefore relevant to test whether the drugs would block depolarisation induced Ca^{2+}-responses. SH-SY5Y cells cultured for 3 days as described above. The Ca^{2+}-response to depolarisation was determined by stimulation with 25 mM – 100 mM K^+ (figure 3-12) and 50 mM was chosen as a suitable concentration. 30 µM verapamil, a well known blocker of VOCC, was used as a positive control (Kohlhardt 1975).

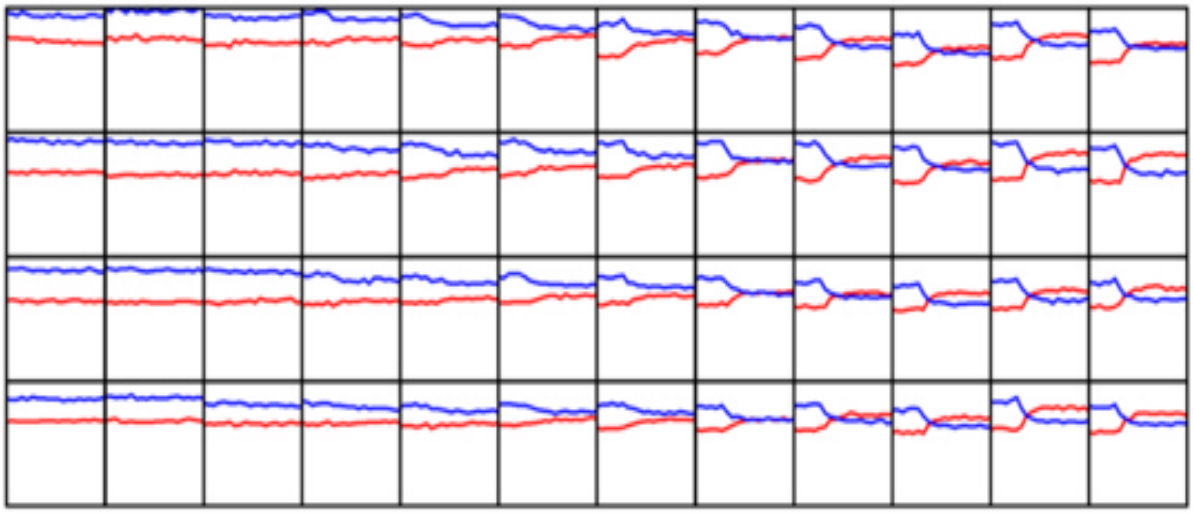

Figure3-12a. Typical "raw data" for single well responses for 48 of the 96 wells in a dose response experiment for calcium responses of SH-SY5Y cells to K^+. Cells were grown for three days on a CellBind multiwell plate and incubated with fura-2 for 45 minutes. Red line is fluorescence at 340 nm (F340), blue line at 380 nm (F380). The increase of F340 and decrease of F380 is a clear indication of intracellular Ca^{2+} rise. Doses of K^+ were (left to right) 0 mM, 25 mM, 30 mM, 35 mM 40 mM, 45 mM, 50 mM, 60 mM, 70 mM, 80 mM, 90 mM, and 100 mM.

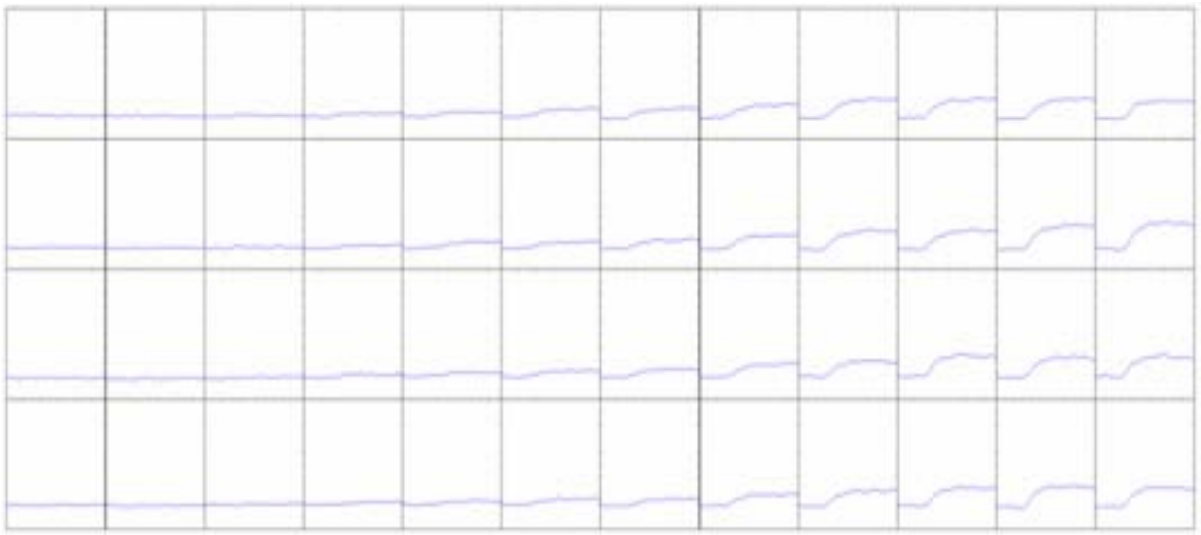

Figure 3-12b Typical ratios for single well responses for 48 of the 96 wells in a dose response experiment for calcium responses of SH-SY5Y cells to K^+. Cells were grown for three days on a CellBind multiwell plate and incubated with fura-2 for 45 minutes. These are the ratios to that corresponds to the data of figure 3-12a Doses were (left to right) 0 mM, 25 mM, 30 mM, 35 mM 40 mM, 45 mM, 50 mM, 60 mM, 70 mM, 80 mM, 90 mM, and 100 mM.

3.6.1 Effect of NMDA-receptor inhibitors on K^+ induced Ca^{2+}-responses

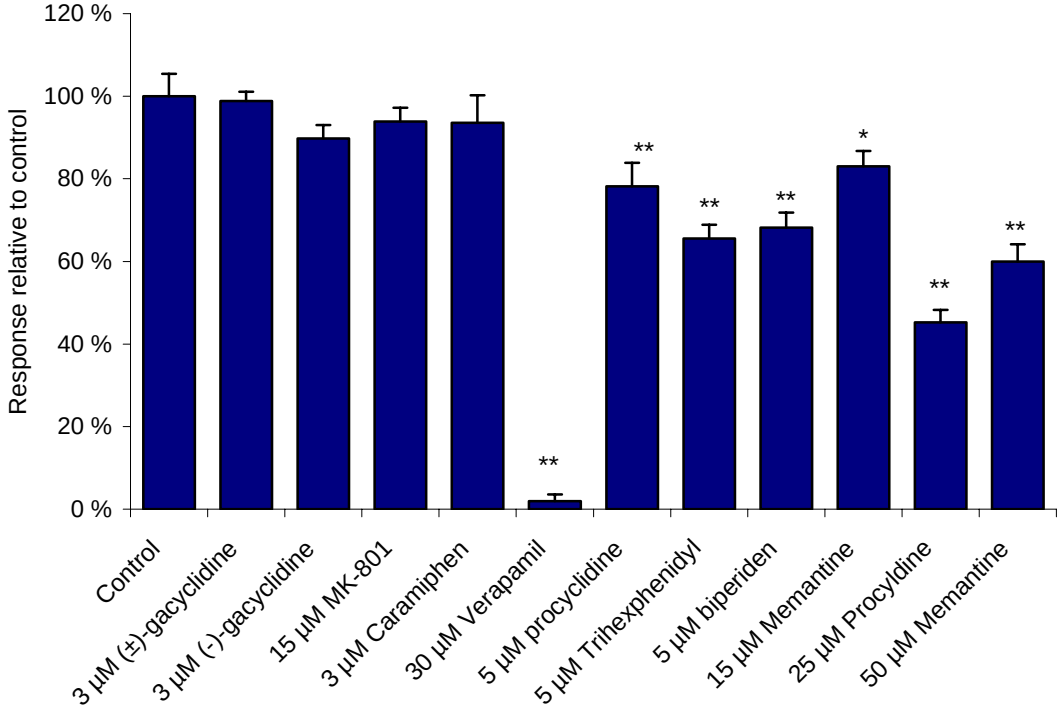

Figure 3-13 Inhibition of K^+ (50 mM) induced Ca^{2+}-responses in the neuroblatoma cell line SH-SY5Y by drugs that block the NMDA-R. Cells were grown for 3 days on a Cellbind multiwell plate and incubated with fura-2 for 45 minutes. Verapamil is a known blocker of VOCC and is used as positive control. Average Ca^{2+}-response with SEM are shown for each drug. All responses were normalised to the response to K^+ without inhibitor (control) taken as 100%. n=8 *p<0.05 ** p<0.01, ANOVA with Dunnett's *post hoc* test.

All the drugs were tested at concentrations high above those needed to block nAChRs. Only the anti-cholinergic Parkinson drugs and memantine significantly blocked the direct depolarisation response. The NMDA-R antagonists gacyclidine and MK-801 did not show any significant block at the concentrations tested (figure 3-**Figure** 13).

3.6.2 Lack of effect of by novel bis-quarternary pyridine compounds on K^+-induced Ca^{2+}-responses

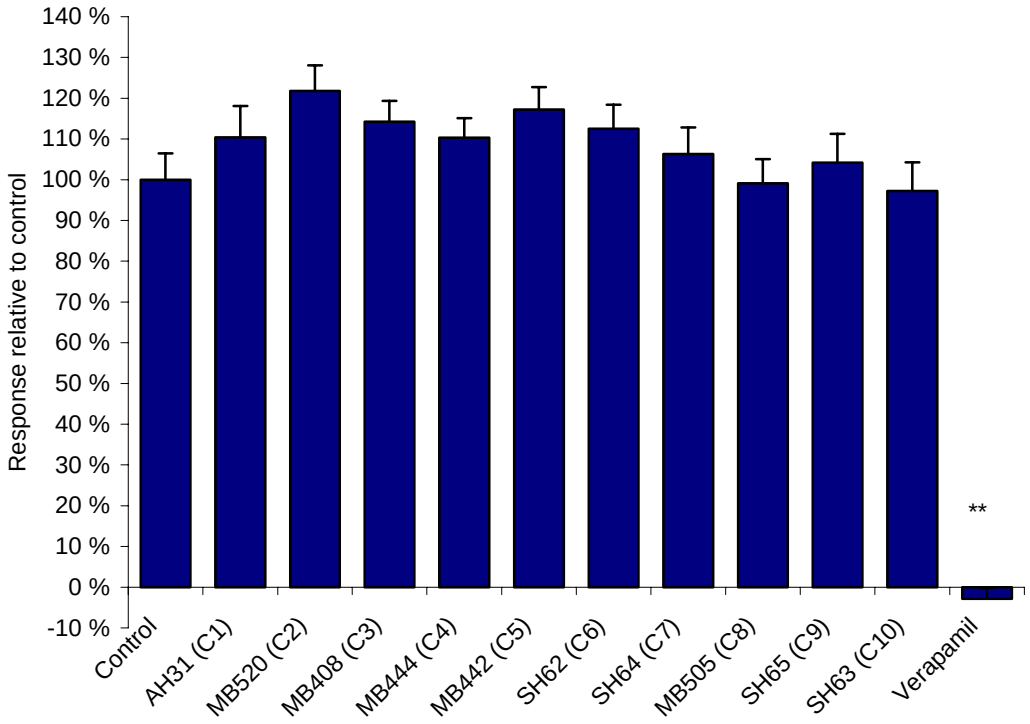

Figure 3-14 Inhibition of K^+ (50 mM) induced Ca^{2+}-responses in the neuroblastoma cell line SH-SY5Y by novel bis-quarternary pyridine compounds. Cells were grown for 3 days ona Cellbind multiwell plate and incubated with fura-2 for 45 minutes. Verapamil is a known blocker of VOCC and is used as positive control. Average Ca^{2+}-response with SEM are shown for each drug. ll responses were normalised to the response to K^+ without inhibitor (control) taken as 100%. n=8. ** $p<0.01$, ANOVA with Dunnett's *post hoc* test.

None of the novel muscle nAChR blockers showed any block of the response at the concentrations tested (figure 3-14). Here the compounds with chain length from 5 to 10 carbon atoms were tested at 100 µM, which is the concentration used as the upper limit for screening for effects on the muscle nAChR (John Tattersall, personal communication). The compounds with chain length from 1 to 4 carbon atoms showed no significant block at nAChR at 100 µM, and therefore testing for effects on VOCC was not relevant. Nevertheless, they were then tested for a possible effect at an even higher concentration (250 µM).

3.6.3 Determination of IC_{50}-values for K^+-induced Ca^{2+}-increase for some NMDA-receptor blockers

For the NMDA-R blockers showing block of K^+-induced Ca^{2+}-increase in the screening, IC_{50}-values were determined by best-fit of the Hill equation. Errors are given as 95% confidence intervals. For memantine the IC_{50} value was 64 µM (31-134 µM). For biperiden, procyclidine and trihexphenidyl the IC_{50} values were 29 µM (22-37 µM), 11.4 µM (8.4-15.5 µM) and 22 µM (16-31 µM), respectively.

3.7 Screening for effects on muscarinic acetylcholine receptors

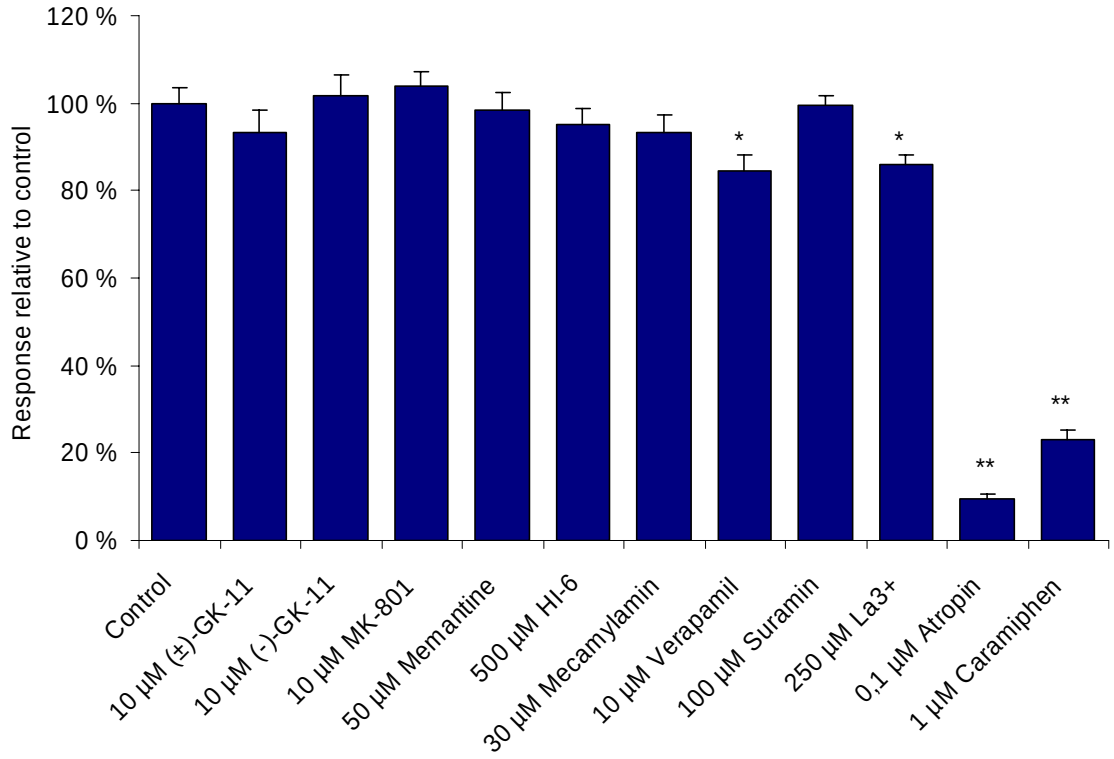

Figure 3-15 Screening of effects on carbachol induced Ca^{2+}-responses in the neuroblastoma cell line SH-SY5Y by drugs that block the NMDA-R. Cells were grown for 3 days on a Cellbind multiwell plate and incubated with fura-2 for 45 minutes. Atropin, a known mAChR antagonist, is used as positive control. The average Ca^{2+}-response with SEM is shown for each drug. The responses were normalised to the response to carbachol without inhibitor (control) taken as 100%. n=8. *$p<0.05$ ** $p<0.01$, ANOVA with Dunnett's *post hoc* test.

The main effects of nerve gas poisoning is attributed to the effects on mAChRs. For drugs to be used against organophosphate poisoning it is therefore relevant to test whether they block the mAchRs of SH-SY5Y. SH-SY5Y cultured for 3 days, were loaded with fluo-3 for these experiments. Fluo-3 offers a higher temporal resolution in the plate reader, which is needed in order to observe these responses properly. Carbachol is an agonist of the mAChR and 5 µM of carbachol was used. Atropin is a classical mAChR antagonist and was the positive control in this experiment. The results are shown in figure 3-15. The only drugs that gave significant block were verapamil, La^{3+} and caramiphen. Verapamil blocks VOCC, while La^{3+} blocks Ca^{2+}-pathways, including ,non specific cation channels. Caramiphen is a known mAChR-antagonist (Hudkins and DeHaven-Hudkins 1991) and atropine is the positive control.

3.8 Screening for effects of NMDA-R blockers on purinergic receptors

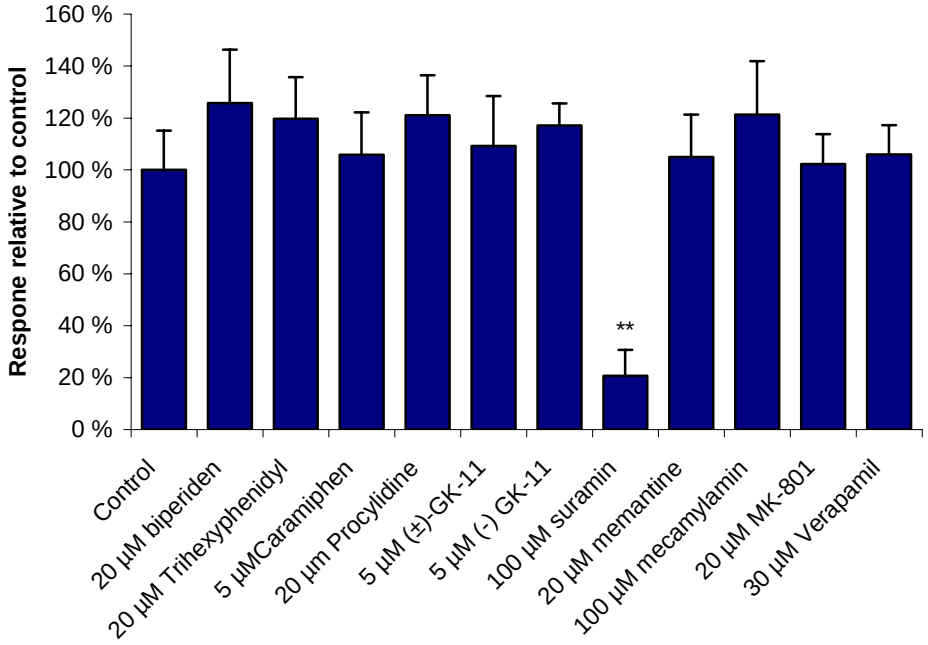

Figure 3-16 Lack of effect by NMDA-R inhibitors on ATP-induced (50 µM) Ca^{2+}-responses in astrocytes by drugs that block the NMDA-R. Cells were grown for 3 days on NUNC multiwell plates and incubated with fura-2 for 1 hour. Suramine is a known P_2-receptor antagonist and is used as positive control. Average Ca^{2+}-response with SEM are shown for each drug. The responses were normalised to the response to ATP without inhibitor (control) taken as 100%. n=8**.** ** $p<0.01$, ANOVA with Dunnett's *post hoc* test.

There were no significant effects of the NMDA-R inhibitors on ATP-induced Ca^{2+}-responses in rat cerebellar astrocytes (figure 3-16). 100µM suramin, a blocker of both P2X and P2Y-receptors, is the positive control. The residual response for suramin is most likely due to mechanical stimulation of the astrocytes.

3.9 Effects on SH-SY5Y response to nicotine by procyclidine and SH63 on membrane potential

Nicotine activates nAChR, and the non-specific increase in cation permeability gives rise to membrane depolarisation. As an additional check for the effects of inhibitor on the neuronal nAChRs, we investigated if nicotine induced changes in single cell responses to membrane potential. The anticholinergic Parkinson drug procyclidine and the bis-quarternary pyridine compund SH63 were tested for their ability to block this reponse. Both procylidine and SH63 blocked the nicotine induced increase in membrane potential. K^+ was used as a positive control in each experiment (figures 3-17 – 3-19).

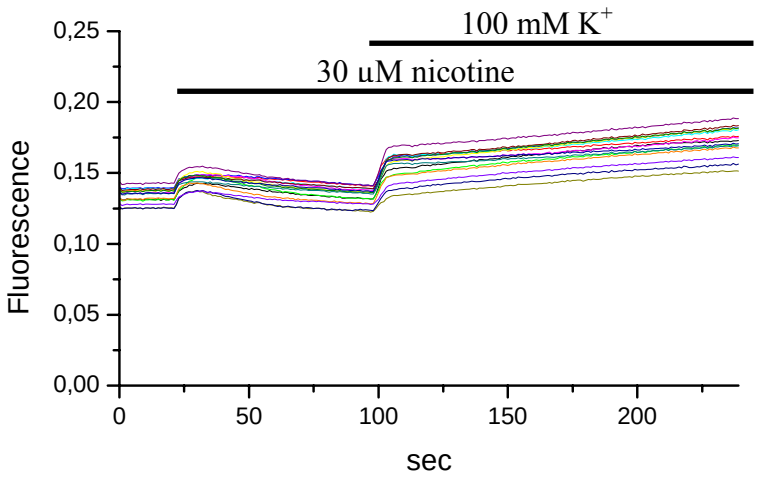

Figure 3-17 Changes in membrane potential in response to 50 µM nicotine and 100 mM K^+ as measured by FMP. The fast increase and subsequent desensitisation after the addition of nicotine is a typical feature of nAChR responses. Cells were grown on glass coverslips for 3 days and incubated with FMP for 30 minutes before the experiment. Fluorescence scale is in arbritary units. 100 mM K^+ represents maximal depolarisation.

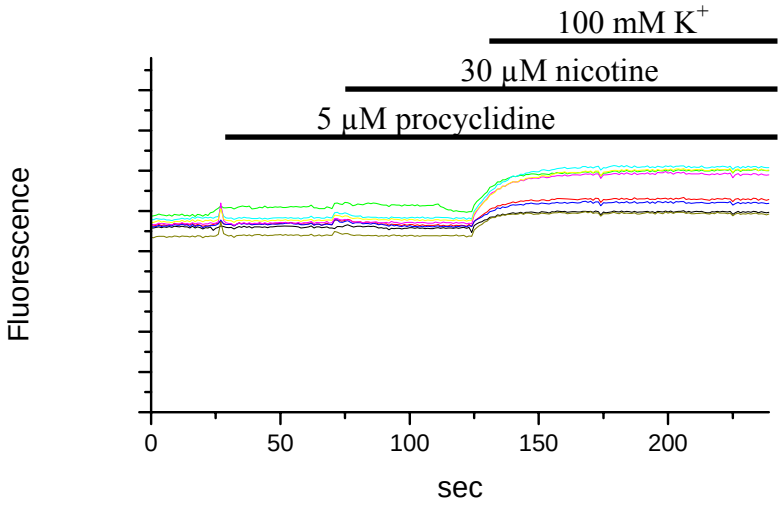

Figure 3-18 Changes in membrane potential in response to nicotine and K^+ after preincubation with 5 µM procyclidine as measured by FMP. Cells were grown on glass coverslips for 3 days and incubated with FMP for 30 minutes before the experiment. Fluorescence scale is in arbritary units. 100 mM K^+ represents maximal depolarisation.

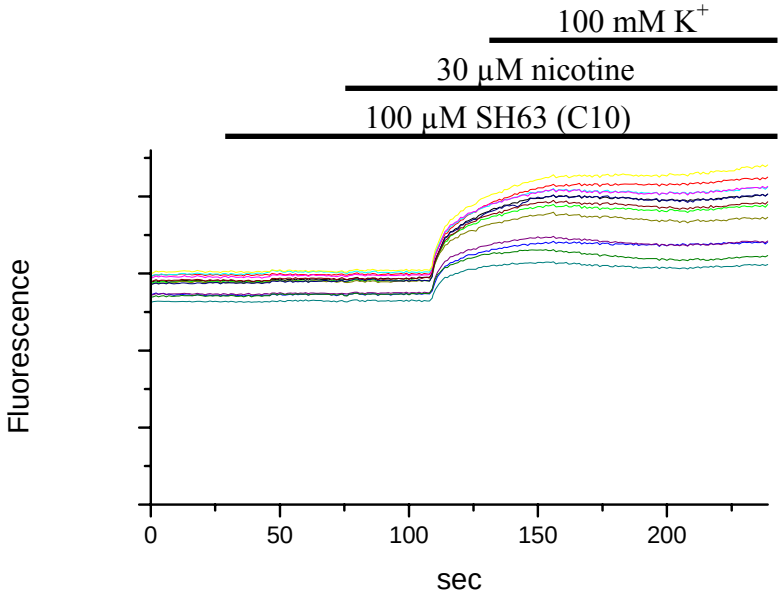

Figure 3-19 Response to nicotine and K^+ after after preincubation with 100 SH-63 as measured by FMP. Cells were grown on glass coverslips for 3 days and incubated with FMP for 30 minutes before the experiment. Fluorescence scale is in arbritary units. 100 mM K^+ represents maximal depolarisation.

4 DISCUSSION

4.1 Evaluation of the method

The main difference between single-cell imaging and measurements with a plate reader is that the plate reader gives much less spatial and temporal resolution than single-cell imaging. Therefore, transient changes in the Ca^{2+}-response are harder to observe with a plate reader. The plate reader, however, allows for automated measurement of many wells, and thus testing of more compounds and more parallels on the same batch of cells. The variability between cells in single-cell imaging will disappear in the plate reader, where each measurement represents the average of response of a large number of cells. As a result of this, the well-to-well varibility is smaller than that between cells in single cell experiments.

As seen from the single cell data, desensitasation of the nAChR is a significant issue even at 30 μM nicotine. This differs from previous data, where a sustained response over 10 minutes was reported after application of 30 μM nicotine (Dajas-Bailador *et al.* 2002). This difference may relate to the higher amounts of dye used in those experiments, or to some difference in the differentiation, subclone of SH-SY5Y or culturing conditions of the SH-SY5Y cell line.

The desensitation is most likely responsible for our observation that the response measured in the plate reader with 50 μM nicotine was slightly greater than the response with 100 μM. With averaged responses, i.e. the cells are not synchronized, a large but faster declining response may appear smaller than a smaller slower declining response. The EC_{50} value obtained from best fit of the Hill equation is probably affected by this. The EC_{50} value of for nicotine stimulated responses on nAChR is 16.8 μM ± 1.5 μM is considerably lower than the value of 43 μM determined by whole-cell patch-clamp (Sokolova *et al.* 2005). This may in part be because desensitasation leads to an underestimate of the maximum response (Y_{max}), and therefore to an underestimate of the value giving half the maximum response (EC_{50}).

The effects of desensitisation on the EC_{50} value for nicotine are not relevant to the determination of the IC_{50} values of the drugs, since in the latter case all experiments were made at the same concentration of nicotine, 50 μM. It should be noted that the method does not discriminate between effects of the drugs on desensitisation and effects on channel gating or permeation. A decreased Ca^{2+} response could, in principle; result from an effect where the drug does not block the channel but instead increases the desensitisation rate. The details of the molecular mechanisms of the nAChR responses, however, were not the aim of this study. For such studies, single cell imaging and patch-clamp data are more appropriate.

There are some concerns in running experiments with fluorescent dyes over a time span of nearly an hour. Extrusion of the dye from the cell may be a significant problem. Therefore, a protocol using fluo-3 would not allow this type of experiment. Fluo-3 is a non-ratiometric dye and a slow drift in the amount of dye would give artefactual changes. Fura-2 is mainly extruded from the cells by the organic anion transporters (Di Virgilio *et al.* 1990). It has been reported that low temperature (Malgaroli *et al.* 1987) or probenecid, an inhibitor of organic anion transporters (Di Virgilio *et al.* 1990), may increase the cytosolic concentration of fura-2 and inhibit its extrusion. For this reason, probenecid was included in all experimental solutions and the temperature was set at 32 °C. It was easier to keep a reproducible temperature at a slightly higher value than room temperature, as the room temperature is not constant in the lab. The other main concern is the transport of probe into intracellular compartments like mitochondria or the ER. There is no simple way of inhibiting this compartmentalisation, although lower temperature slows uptake intracellular compartments. For these reasons, only 48 wells were initially run, but as there were no significant differences between experiments with 48 and 96 wells, 96 well were used in the final method.

4.1.1 Validating the method

The method uses the indirect consequences of nAChr channel opening and cell membrane depolarisartion. One concern was that the block obtained from the drugs was a block of Ca^{2+}-responses downstream to the activation of nAChr, and not an indication of the block of nAChR themselves. The nAChr activation results in a rise in $[Ca^{2+}]_i$ which is partly due to influx of Ca^{2+} through the nAChr, but is also due to a secondary rise in $[Ca^{2+}]_i$ which comes as a consequences of Ca^{2+} and Na^+ influx. In Ca^{2+} responses of excitable as well as inexcitable cells there are generally a number of phases of calciunm change, starting with a fast peak in Ca^{2+}. For example, IP_3 and CICR (see section 1.2.2) mediated responses are transient phenomena which typically give a peak in Ca^{2+} that starts already after fractions of a second and lasts for a few seconds. In the method used here we intentionally measure later responses, more than 10 seconds after nicotine stimulation, that correspond to the sustained phase of the response to nicotine, when the transient peak has already decayed (Berridge and Bootman 1998).

To test for effects of drugs on the non-desensitizing voltage operated calcium channels (VOCC), K^+ was used to depolarise the cells and drugs were used at values much higher than their IC_{50} to screen for effects on the depolarisation induced calcium influx. No block of the K^+-induced calcium influx was seen at relevant concentrations consistent with the interpretation that the block seen is that of the nAChR and not of the downstream recruitment due to the depolarisation. Memantine has previously been shown to block nAChR with IC_{50} values from 0.3 to 7 μM, depending on the subtype and tissue model used. Mematine was also shown to block the different nAChR in a use-dependent and voltage-dependent manner (Buisson and Bertrand 1998; Maskell *et al.* 2003; Aracava *et al.* 2005). It is therefore a suitable control for the use-dependent and voltage dependent block of nAChR. The IC_{50} value of 2.85 μM obtained for memantine is in the middle of the range of the previously reported data. In addition, the method reproduced the use-dependent and voltage-dependent block of nAChr by memantine, a result which demonstrates the usefulness and validity of the method.

To further test the consistency of the results, a single cell imaging experiment was run to test for block of nicotine stimulated depolarisation with the aid of the membrane

potential probe. This measurement is mainly dependent on Na^+-influx through nAChr and not on secondary recruitment of intracellular Ca^{2+}. Procyclidine blocked the nicotine-induced change in membrane potential consistent with the conclusions, from the measurements with fura-2, that anticholinegic Parkinson drugs block the nAChr. It may be noted that FMP is not as suitable as fura-2 in plate reader experiments because it is not ratiometric and the signal changes with time.

4.1.2 Further improvement of the method

The method is well suited for screening drugs for general effects on nAChR. A limitation with the cell model used here, and similarly with any cell line expressing more than one subtype of nAChR, is that the protocol used does not discriminate between the different subtypes of nAChRs. Currently, no method exists to screen for effects on different subtypes. The most frequently used method for studying single subtypes of nAChRs is hetrologous expression in oocytes or in cell lines (Buisson and Bertrand 1998; Kishi and Steinbach 2006). Although oocytes are not suitable for screening, a cell line model would be suitable if the nAChR is stably expressed. In general this is not easily attainable. Instead, one possible approach could be to attempt to block the specific receptors with selective blockers. The main nAChRs in SH-SY5Y are α3β2 and α7-receptors (Dajas-Bailador *et al.* 2002). Therefore, selective blockers for these receptors may be useful to block out the contribution of either receptor, e.g. using α-bungraotoxin to block α7-receptors or α-conotoxin MII to block α3β2-receptors (Dajas-Bailador *et al.* 2002). Extension of the method in this direction will be attempted in future work but was not attainable within the scope of the present thesis.

4.2 Anticholinergic Parkinson drugs

One of the objectives of the thesis was to determine the possible inhibition of nAChRs by anticholinergic Parkinson drugs. Trihexphenidyl was the most potent of the anti-cholinergic Parkinson drugs at the nAChR-response and about twice as potent as biperiden and procyclidine, which are approximately equipotent. This does not correlate well with their potencies at the NMDA-R, where procylidine is about 15 times more potent (i.e. has 15 times lower IC_{50}) than biperiden and trihexphenidyl. Procyclidine is about twice as potent at nAChR as at NMDA-R, while biperiden and trihexphenidyl are about 30 and 60 times, respectively, more potent on nAChR than on NMDA-R. Even though procyclidine is the least potent of the drugs on mAChRs, it is still about 20 times more potent on the mAChR than on the nAChR. Biperiden and trihexphenidyl are approximately 180 and 30 times more potent on mAChR than on nAChR (Syvälahti *et al.* 1988). All these drugs also blocked VOCC, but at concentrations at least 10 times higher than the ones needed to block nAChR, and the block of nAChR seen is therefore not significantly affected by block of VOCC. However, biperiden and trihexphenidyl blocks the NMDA-R with potencies similar to that of VOCC (Ring and Tansø, unpublished data). To summarise, the relative potencies for block of mAChR are biperiden > trihexphenidyl > procyclidine (Syvälahti *et al.* 1988), for nAChR trihexphenidyl > procyclidine ≈ biperiden and for NMDA-R procyclidine >> biperiden ≈ trihexphenidyl.

4.2.1 Use- and voltage-dependence

A use dependent manner of block ideally allows for the normal activity of the receptor, while blocking the higher activity of receptors. This may be relevant for conditions like ischemic brain damage (excessive glutamate receptor activation) and brain seizures due to organophosphate poisoning (excessive cholinergic activation). The picture is complicated by the fact that some manner of use-dependence, in particular open-channel block, can inhibit the desensitsation of the receptor, and thus increase the total activity of the receptor (Alkondon and Albuquerque 1989). Voltage dependent block may be seen as a variant of use dependence, where the overall activity of the cell, as set by its membrane potential, controls the blocking activity of the inhibitor. Both biperiden and trihexphenidyl showed a significant use dependent block. Procyclidine did not show significant use dependence, but it showed voltage

dependence. As the structure of these anticholinergic Parkinson drugs are very similar, it is diffucult to see that one would block in a non-use dependent manner, while the others do. The negative result for procyclidine may be attributed to a lack of sensitivity of the method. In comparison, the block of nAChR by procyclidine was voltage dependent, and biperiden and trihexphenidyl were not tested. It is probable that all the anticholinergic Parkinson drugs block the nAChR in a use and voltage dependent manner, although further experiments are needed to clarify this.

4.2.2 Pharmacokinetic aspects of block by anticholinergic Parkinson drugs

It would be valuable to extend the present work with measurement of the brain uptake of the drugs, since these data are not found in the literature, except for biperiden. Nevertheless, from the available pharmacokinetic data, we may try to estimate the brain concentrations of the anticholinergic Parkinson drugs. The plasma concentration of the drugs after intravenous injection of a single dose may be calculated from the equation:

$C(mol/L) = \frac{dose(mol/kg)}{V_d(L/kg)}$, where V_d is the apparent volume of distribution (Benet *et al.* 1995). Using this equation and the values given by Brocks (1999) (for values, see section 1.7.1), the plasma concentration of biperiden corresponding to the ED_{50} against soman-posioning in rat (Shih *et al.* 1999) after 5 and 40 minutes are 12.0 nM and 2.55 μM, respectively. This is assuming that the V_d are the same in rat and human. Since the concentrations in the brain are 10 times the plasma concentration (Yokogawa *et al.* 1992), the corresponding brain concentrations are 0.12 μM and 25.5 μM. There is general agreement that block of mAChR is the dominant mechanism for stopping seizures 5 minutes after soman exposure. The concentration after 5 minutes is therefore expected to be of a magnitude consistent with the IC_{50} value for block of mAChR. This is in agreement with the value of 0.12 μM estimated above. This value is also a factor of 10 below the IC_{50} of biperiden on nAChR-responses and a factor 400 below the IC_{50} for NMDA-R (Ring and Tansø, unpublished data), also consitent with the consensus that after 5 minutes only the mAChR are involved.

It is reasonable to assume that the concentrations of the drugs in the brain required to stop seizures are proportional to the respective IC_{50} values on mAChR. As no data relating to the partition of procyclidine or trihexphenidyl is available, these have to be estimated. If we assume the brain concentration calculated above for biperiden and use the IC_{50} of biperiden at mAChR (Syvälahti *et al.* 1988) we can calculate the ratio between the brain concentration and the IC_{50} for biperiden:

$$ratio = \frac{C_{brain}}{IC_{50}} = \frac{0.12\mu M}{0.0084\mu M} = 14.3$$

If this ratio is valid also for other anti-muscarinic drugs, e.g. procyclidine, then the brain concentration of procyclidine 5 minutes after soman poisoning is:

$$C_{brain} = ratio \cdot IC_{50} = 14.3 \cdot 0.070\mu M = \underline{1.0\mu M}$$

If we assume that the concentration in the brain is proportional to the dose given then the concentration corresponding to the ED_{50} after 40 minutes (Shih *et al.* 1999) is

$$C_{brain}(40) = \frac{ED_{50}(40)}{ED_{50}(5)} \cdot C_{brain}(5) = \frac{13.3mg/kg}{1.51mg/kg} \cdot 1.0\mu M = 8.8\mu M$$

These calculations estimate the brain concentrations of procyclidine corresponding to ED_{50} against soman-induced seizures 5 and 40 minutes after soman-poisoning to be 1.0 μM and 8.8 μM, respectively. If we do the same calculations for trihexphenidyl the corresponding values are 0.4 μM and 14 μM.

With the above assumptions, we may now conclude that, the concentrations 40 minutes after soman-induced seizures in the brain correspond to concentrations where the nAChR-responses are completely blocked, while the NMDA-R are only partially inhibited. Nevertheless, since the concentration of drug in different parts of the brain may vary (Yokogawa *et al.* 1992), it may be that the inhibitions both of NMDA-R and of nAChR influence the effects against soman at the late stage. The brain concentration of procyclidine 5 minutes after soman exposure is expected to have effects on nAChR and on NMDA-R as well. The above calculated brain concentration of procyclidine after 5 minutes may therefore be overestimated as the inhibition of nAChR and NMDA-R may reduce the amount of mAChR block required to stop seizures. The narrower range of IC_{50} values for procyclidine at the different receptor

types may actually make procyclidine more useful as it may help against other symptoms of the OP poisoning than only the muscarinic.

For nicotine-induced seizures (Gao *et al.* 1998) the potencies are similar for all three drugs. The brain concentrations for the anticholinergic Parkinson drugs at the ED_{50}, calculated as described above, are 6 μM, 2 μM and 7 μM for biperiden, procyclidine and trihexphenidyl. These data indicate that both NMDA-R and nAChR may be significant in these seizures, which is reasonable as nicotine may stimulate the release of glutamate in the CNS (Jensen *et al.* 2005). Indeed the report by Gao *et al.* (1999) does not identify nAChR as the target of the anti-seizure effects, but leaves open the question whether the anti-seizure effects are effects at NMDA-R.

4.3 Memantine

As discussed above (section 4.1.1), the data for memantine on the nAChR correspond well to the available data from the literature (Buisson and Bertrand 1998; Maskell *et al.* 2003; Aracava *et al.* 2005). Memantine alone does not stop soman-induced seizures, neither after 5 minutes nor after 40 minutes. This may be partially due to its lack of anti-muscarinic activity, but may also be due to the rapid dissociation of memantine from the NMDA-R (Parsons *et al.* 1999). The experiments on soman induced seizures were done without any centrally acting anti-muscarinic agent, and it may be that memantine, similar to gacyclidine (Lallement *et al.* 1997), may be useful if given in addition to atropine and an oxime.

4.4 Gacyclidine and MK-801

MK-801 blocked the nicotine induced Ca^{2+}-response with an IC_{50} of 1.80 µM. This is much lower than the values obtained for isolated receptors in hetorologous expression systems (Buisson and Bertrand 1998). This may be due to a different affinity for the different subtypes of receptors, and the IC_{50} of MK-801 to α3β2-receptors is not known. Another explanation may be that the measured affinity may differ in different systems. This is similar to memantine, where the observed IC_{50} values varies 20 fold between hippocampal neurons and an oocyte expression system (Maskell *et al.* 2003; Aracava *et al.* 2005). MK-801 showed neither voltage dependence nor use dependence. The conclusion from our experiments for nAChR is consistent with earlier reports (Briggs and McKenna 1996; Buisson and Bertrand 1998).

Only a small difference in IC_{50} was seen between racemic gacyclidine and (-)-gacyclidine at the nAChR. This is similar to what is seen for the NMDA-R, where, surprisingly, no difference is seen between the racemate and the pure isomer. This was concluded in studies on NMDA-R (Ring and Tansø, unpublished data) and recently confirmed independently (Helene Hirbec, private communication) and in models of neurotoxicity (Drian *et al.* 1999). In both cases, however, differences are seen between the pure isomers. (-)-gacyclidine showed a use-dependent manner of block, while the results for the racemate was not significant. This may be due to a lack of sensitivity in the method, or it may be that there is a difference in the manner of block between the different isomers. The (+) isomer was not available for testing in this study.

4.4.1 nAChR may be the "non-NMDA" binding sites of gacyclidine

The non-NMDA binding sites in rat brain has been described in two reports (Hirbec *et al.* 2001c, 2001b). The binding was described as uniform in the forebrain and a more discrete distribution in the cerebellum. The authors did not succeed in identifying the site, and no target was suggested , but interestingly we now observe that the distribution reported for this site is in fairly good accordance with the distribution of nAChR in the CNS (Gotti and Clementi 2004). This data, together with our finding that gacyclidine blocks the nAChR, makes the nAChRs a good candidate for these "non-NMDA" binding sites of gacyclidine.

4.4.2 Clinical relevance of gacyclidine

It was claimed that gacyclidine shows less neurotoxixity than classical NMDA-R antagonists like MK-801 (Hirbec *et al.* 2001a). It has been shown to be neuroprotective in several different animal and human studies (Lallement *et al.* 1997; Lepeintre *et al.* 2004; Fehlings and Baptiste 2005). It was suggested that the "non-NMDA" binding sites may account for the difference in the neurotoxicity between gacyclidine and other NMDA-R antagonists (Hirbec *et al.* 2001c). This hypotheis may implicate the relevance of nAChR in the neuroprotective effects of gacyclidine.

4.5 Caramiphen

Caramiphen blocks the nAChR-response with an IC_{50} that is two orders of magnitude lower than for NMDA-R (Ring and Tansø, unpublished data). Its potency at the mAChR (Hudkins *et al.* 1991), in turn, is two orders of magnitude higher than that at the nAChR. These data strongly suggest that caramiphen is effective only through its antimuscarinic effects. This is consistent with the observation that caramiphen does not stop soman-induced seizures after 40 minutes, but stops seizures 5 minutes after soman exposure (Shih *et al.* 1999). Nevertheless, it appears to be more effective than scopolamine, a pure mAChR antagonist (Raveh *et al.* 2002) and this may be due to its additional effects at the nAChR.

4.6 Novel bis-quarternary pyridine compounds

There seems to be a clear relationship between the chain length of these drugs, and their potency at the neuronal nAChR-receptors, with the longer chain lengths giving an increased block. The drugs with a chain-length from 1-3 carbon atoms gave no block at 100 μM, which is a maximal concentration considered relevant for these drugs. With the drugs with chain lengths from 4 to 10 carbon atoms the IC_{50} values were monotonically decreasing. This was completely unexpected since the corresponding relationship between response and chain length for the muscle nAChR is bell-shaped, with a maximum block for a 5 carbon chain, and less block for longer or shorter chain-lengths (John Tattersall, personal communication). It is interesting to note that the classical ganglionic open-channel blocker hexamethonium has a 6 carbon chain between two positive charges.

Our data indicate a use-dependent mechanism for block for SH63 (chain length 10). Since use-dependence in the present case is associated with open-channel block, this is somewhat surprising. (+)-tubocurarine is a known competitive antagonist for neuronal and muscle nAChR (Dwoskin and Crooks 2001), and (+)-tubocurarine has a similar structure to SH63 with regard to the classical structure-activity relationship at nAChRs. At the muscle nAChR SH63 also seems to block in a competitive manner as seen by the results on guinea pig diaphragm (John Tattersall, personal communication). It should be noted, however, that the nAChRs are classical models for allosteric interactions (Lena and Changeux 1993), and the blocking action of SH63 may be a result of mixed competitive and non-competitive blocking actions. Another possibility is that the IC_{50} values of different nAChR subtypes are sufficiently different to give rise to an apparent non-competitive block. Further studies may resolve this.

The clinical relevance of these observations remains to be clarified. The relevant maximal blood plasma concentration is thought to be about 100 μM (Tattersall 1993). Since all these compounds have two positive charges they are unlikely to cross the blood-brain barrier well enough to give a significant concentration in the brain. Therefore, their effect on the CNS is dependent on special pharmaceutical formulations or the delivery of these drugs in the form of pro drugs, which might reduce their effect on the muscle nAChR. The autonomous ganglia, however, are located outside the blood-brain barrier and these compounds may alleviate the symptoms of OP poisoning caused by excessive activation of the autonomic nervous system, including hypertension and tachycardia. In addition, the novel synthetic pyridines were synthesized primarily with intention to target muscle nAChr. It is therefore important to take into account the action of the drugs also at the ganglia when selecting the most apropriate drug to use. Our data help in discriminating between the drugs and suggest that one might choose a lesser potent blocker (i.e. a shorter length pyridine) in order to minimize effects on the autonomic nervous system.

CONCLUSIONS

The screening method developed was convenient and efficient in screening different compounds for their inhibitory action at nAChR. It also proved reliable in characterising different types of block as well as the amount (i.e. the IC_{50}) of block. The robustness of the method suggests that it may be further refined and applied to quantify subtypes of nAChR, although coexpressed in the same cell line.

The anti-cholinergic Parkinson drugs procyclidine, biperiden and trihexphenidyl blocked the nAChR-response in a use and voltage dependent manner. Although these drugs are closely related in chemical structure, there is little correlation between their relative potencies at nAChr, mAChR and NMDA-R. The IC_{50} are in the order mAChR < nAChR < NMDA-R for all three drugs. The abundance of nAChR in the CNS, taken together with the relative high potencies at nAChR, suggests a role for the effects of the drugs at nAChR in the inhibition of organophosphate-induced seizures.

Gacyclidine also blocks nAChR-responses in a use dependent manner. Both the racemate and the (-)-isomers are about 10 times less potent at nAChR than at NMDA-R, which distinguishes gacyclidine from the anticholinergic Parkinson drugs. The finding that gacyclidine blocks the nAChR-response and the observation that the distribution of the“non-NMDA” binding sites for gacyclidine correlates with the expression of nAChR in the CNS, suggests that these are identical. Further studies should be undertaken to clarify this hypothesis.

The novel bis-quarternary pyridine compounds block nAChR. The structure-activity relationship indicates that, for the range of chain length in this study, C1 to C10, the inhibiting potency increases with chain-length of the linker between the pyridine rings. This is in contrast to the data on muscle nAChR, where a 5 carbon linker had the highest potency. These data should be taken into consideration when choosing the compound to develop as an oxime or inhibit muscle nAChR, since a potent block of ganglionic nAChR may not be desirable. On the other hand, if oxime delivery to the CNS is desirable, e.g when the blood brain barrier is compromised, then the longest chain, C10, would be the candidate of choice.

REFERENCES

Alberts B., Johnson A., Lewis J., Raff M., Roberts K. and Walter P. (2002) *Molecular Biology of the cell*. Garland Science, New York.

Alkondon M. and Albuquerque E. X. (1989) The nonoxime bispyridinium compound SAD-128 alters the kinetic properties of the nicotinic acetylcholine receptor ion channel: a possible mechanism for antidotal effects. *The Journal of pharmacology and experimental therapeutics* **250,** 842-852.

Aracava Y., Pereira E. F., Maelicke A. and Albuquerque E. X. (2005) Memantine blocks alpha7* nicotinic acetylcholine receptors more potently than n-methyl-D-aspartate receptors in rat hippocampal neurons. *The Journal of pharmacology and experimental therapeutics* **312,** 1195-1205.

Barlow R. and Blake J. F. (1989) Hill coefficients and the logistic equation. *Trends in Pharmacological Sciences* **10,** 440-441.

Barthold C. L. and Schier J. G. (2005) Organic phosphorus compounds - nerve agents. *Critical care clinics* **21,** 673-689.

Baxter D. F., Kirk M., Garcia A. F., Raimondi A., Holmqvist M. H., Flint K. K., Bojanic D., Distefano P. S., Curtis R. and Xie Y. (2002) A novel membrane potential-sensitive fluorescent dye improves cell-based assays for ion channels. *Journal of biomolecular screening* **7,** 79-85.

Benet L. Z., Kroetz D. L. and Sheiner L. B. (1995) Pharmacokinetics, in *Goodman & Gilman's The Pharmacological Basis of Theraputics,* 9th Edition, pp 503-519. McGraw-Hill, New York.

Berridge M. J. (1998) Neuronal calcium signaling. *Neuron* **21,** 13-26.

Berridge M. J. and Bootman M. D. (1996) Calcium signaling in *Signal Transduction* (Heldin C.-H. and Purton M., eds), pp 205-222. Clapman & Hall, London.

Bertrand D. (2005) The possible contribution of neuronal nicotinic acetylcholine receptors in depression. *Dialogues in clinical neuroscience* **7,** 207-216.

Bhagat Y. A., Obenaus A., Hamilton M. G., Mikler J. and Kendall E. J. (2005) Neuroprotection From Soman-induced Seizures In The Rodent: Evaluation With Diffusion- And T2-weighted Magnetic Resonance Imaging. *Neurotoxicology* **26,** 1001-1013.

Biedler J. L., Helson L. and Spengler B. A. (1973) Morphology and growth, tumorigenicity, and cytogenetics of human neuroblastoma cells in continuous culture. *Cancer research* **33,** 2643-2652.

Bird G. S. and Putney J. W. (2006) Calcium, in *Basic Neurochemistry,* 7th Edition (Siegel G. J., Albers R. W., Brady S. T. and Price D. L., eds), pp 267-290. Elsvier Academic Press, London.

Briggs C. A. and McKenna D. G. (1996) Effect of MK-801 at the human alpha 7 nicotinic acetylcholine receptor. *Neuropharmacology* **35,** 407-414.

Brisson A. and Unwin P. N. (1984) Tubular crystals of acetylcholine receptor. *The Journal of cell biology* **99,** 1202-1211.

Brocks D. R. (1999) Anticholinergic drugs used in Parkinson's disease: An overlooked class of drugs from a pharmacokinetic perspective. *Journal of Pharmacy & Pharmaceutical Sciences* **2,** 39-46.

Buckley N. A., Karalliedde L., Dawson A., Senanayake N. and Eddleston M. (2004) Where is the evidence for treatments used in pesticide poisoning? Is clinical toxicology fiddling while the developing world burns? *Journal of toxicology. Clinical toxicology.* **42,** 113-116.

Buisson B. and Bertrand D. (1998) Open-channel blockers at the human alpha4beta2 neuronal nicotinic acetylcholine receptor. *Molecular pharmacology* **53,** 555-563.

Burnstock G. (2006) Purinergic signalling - an overview. *Novartis Foundation symposium* **276,** 26-57.

Dajas-Bailador F. and Wonnacott S. (2004) Nicotinic acetylcholine receptors and the regulation of neuronal signaling. *Trends in Pharmacological Sciences* **25,** 317-324.

Dajas-Bailador F. A., Mogg A. J. and Wonnacott S. (2002) Intracellular Ca^{2+} signals evoked by stimulation of nicotinic acetylcholine reseptors SH-SY5Y cells: contribution of voltage-operated Ca^{2+} channels and Ca^{2+} stores. *Journal of Neurochemistry* **81,** 606-614.

Di Virgilio F., Steinberg T. H. and Silverstein S. C. (1990) Inhibition of Fura-2 sequestration and secretion with organic anion transport blockers. *Cell Calcium* **11,** 57-62.

Drian M. J., Kamenka J. M. and Privat A. (1999) In vitro neuroprotection against glutamate toxicity provided by novel non-competitive N-methyl-d-aspartate antagonists. *Journal of Neuroscience Research* **57,** 927-934.

Dunlap K., Luebke J. I. and Turner T. J. (1995) Exocytotic Ca^{2+} channels in mammalian central neurons. *Trends in Neuroscience* **18,** 89-98.

Dwoskin L. P. and Crooks P. A. (2001) Competitive neuronal nicotinic receptor antagonists: a new direction for drug discovery. *The Journal of pharmacology and experimental therapeutics* **298,** 395-402.

Fehlings M. G. and Baptiste D. C. (2005) Current status of clinical trials for acute spinal cord injury. *Injury* **36 Suppl 2,** B113-122.

Foster A. C. and Wong E. H. (1987) The novel anticonvulsant MK-801 binds to the activated state of the N-methyl-D-aspartate receptor in rat brain. *British journal of pharmacology* **91,** 403-409.

Gao Z. G., Liu B. Y., Cui W. Y., Li L. J., Fan Q. H. and Liu C. G. (1998) Anti-nicotinic properties of anticholinergic antiparkinson drugs. *Journal of Pharmacy & Pharmacology* **50,** 1299-1305.

Gotti C. and Clementi F. (2004) Neuronal nicotinic receptors: from stucture to pathology. *Progress in Neurobioology* **74,** 363-396.

Gotti C., Zoli M. and Clementi F. (2006a) Brain nicotinic acetylcholine receptors: native subtypes and their relevance. *Trends in pharmacological sciences* **27,** 482-491.

Gotti C., Riganti L., Vailati S. and Clementi F. (2006b) Brain neuronal nicotinic receptors as new targets for drug discovery. *Current pharmaceutical design* **12,** 407-428.

Grynkiewicz G., Poenie M. and Tsien R. Y. (1985) A new generation of Ca2+ indicators with greatly improved fluorescence properties. *The Journal of biological chemistry* **260,** 3440-3450.

Harrison P. K., Sheridan R. D., Green A. C., Scott I. R. and Tattersall J. E. (2004) A guinea pig hippocampal slice model of organophosphate-induced seizure activity. *The Journal of pharmacology and experimental therapeutics* **310,** 678-686.

Hassel B. (2006) Nicotinic mechanisms contribute to soman-induced symptoms and lethality. *Neurotoxicology* **27,** 501-507.

Hassel B. and Dingledine R. (2006) Glutamate, in *Basic Neurochemistry*, 7th Edition (Siegel G. J., Albers R. W., Brady S. T. and Price D. L., eds), pp 267-290. Elsvier Academic Press, London.

Heacock A. M. and Fisher S. K. (2006) Phosphinositides, in *Basic Neurochemistry,* 7th Edition (Siegel G. J., Albers R. W., Brady S. T. and Price D. L., eds), pp 347-360. Elsvier Academic Press, London.

Hertz L., Juurlink B. H., Hertz E., Fosmark H. and Schousboe A. (1989) Preparation of primary cultures of mouse (rat) astrocytes, in *A dissection and tissue culture*

manual for the nervous system (Shahar A., Vellis J. d., Vernandakis A. and haber B., eds), pp 105-108. Alan R. Liss, New York.

Hirbec H., Gaviria M. and Vignon J. (2001a) Gacyclidine: a new neuroprotective agent acting at the N-methyl-D-aspartate receptor. *CNS drug reviews* **7,** 172-198.

Hirbec H., Kamenka J. M., Privat A. and Vignon J. (2001b) Interaction of gacyclidine enantiomers with 'non-NMDA' binding sites in the rat central nervous system. *Brain research* **894,** 189-192.

Hirbec H., Kamenka J. M., Privat A. and Vignon J. (2001c) Characterization of 'non-N-methyl-D-Aspartate' binding sites for gacyclidine enantiomers in the rat cerebellar and telencephalic structures. *Journal of neurochemistry* **77,** 190-201.

Hudkins R. L. and DeHaven-Hudkins D. L. (1991) M1 muscarinic antagonists interact with sigma recognition sites. *Life sciences* **49,** 1229-1235.

Hudkins R. L., DeHaven-Hudkins D. L. and Stubbins J. F. (1991) Muscarinic receptor binding profile of para-substituted caramiphen analogues. *Journal of medicinal chemistry* **34,** 2984-2989.

Invitrogen (2006) Chapter 19 — Indicators for Ca{2+}, Mg{2+}, Zn{2+} and Other Metal Ions, in *The Handbook — A Guide to Fluorescent Probes and Labeling Technologies*

Jenkinson D. H. (2002) Classical approaches to the study of drug-receptor interaction, in *Textbook of receptor pharmacology,* 2nd Edition (Foreman J. C. and Johansen T., eds), pp 3-72. CRC Press LCC.

Jensen A. A., Frolund B., Liljefors T. and Krogsgaard-Larsen P. (2005) Neuronal nicotinic acetylcholine receptors: structural revelations, target identifications, and therapeutic inspirations. *Journal of medicinal chemistry* **48,** 4705-4745.

Kao J. P. Y. (1994) Practical aspects of measuring [Ca^{2+}] with fluorescent indicators, in *Methods in cell biology: A practical guide to the study of Calcium in living cells* (Nuccitelli R., ed.), pp 155-181. Academic Press Inc., San Diego, CA, USA.

Kishi M. and Steinbach J. H. (2006) Role of the agonist binding site in upregulation of neuronal nicotinic {alpha}4{beta}2 receptors. *Molecular Pharmacology***,** mol.106.029298.

Kohlhardt M. (1975) Functional differentiation of the transmembrane sodium and calcium channels in mammalian cardiac fibers by use of specific inhibitors. *Recent advances in studies on cardiac structure and metabolism* **5,** 19-26.

Kornhuber J. and Quack G. (1995) Cerebrospinal fluid and serum concentrations of the N-methyl-D-aspartate (NMDA) receptor antagonist memantine in man. *Neuroscience Letters* **195,** 137-139.

Lallement G., Mestries J. C., Privat A., Brochier G., Baubichon D., Carpentier P., Kamenka J. M., Sentenac-Roumanou H., Burckhart M. F. and Peoc'h M. (1997) GK 11: promising additional neuroprotective therapy for organophosphate poisoning. *Neurotoxicology* **18,** 851-856.

Lambert D. G., Ghataorre A. S. and Nahorski S. R. (1989) Muscarinic receptor binding characteristics of a human neuroblastoma SK-N-SH and its clones SH-SY5Y and SH-EP1. *European journal of pharmacology* **165,** 71-77.

Lena C. and Changeux J. P. (1993) Allosteric modulations of the nicotinic acetylcholine receptor. *Trends in neurosciences* **16,** 181-186.

Lepeintre J. F., D'Arbigny P., Mathe J. F., Vigue B., Loubert G., Delcour J., Kempf C. and Tadie M. (2004) Neuroprotective effect of gacyclidine. A multicenter double-blind pilot trial in patients with acute traumatic brain injury. *Neurochirurgie* **50,** 83-95.

Linden J. and Rosin D. L. (2006) Purinergic system, in *Basic Neurochemistry,* 7th Edition (Siegel G. J., Albers R. W., Brady S. T. and Price D. L., eds), pp 303-316. Elsevier Academic Press, London.

Lipton S. A. and Rosenberg P. A. (1994) Excitatory amino acids as a final common pathway for neurologic disorders. *The New England journal of medicine* **330,** 613-622.

Lukas R. J., Norman S. A. and Lucero L. (1993) Characterization of nicotinic acetylcholine receptors expressed by cells of the SH-SY5Y human neuroblastoma clonal line. *Molecular and Cellular Neuroscience* **4,** 1-12.

Lundbeck A/S 2006 Summary of product charachteristics: Ebixia

Malgaroli A., Milani D., Meldolesi J. and Pozzan T. (1987) Fura-2 measurement of cytosolic free Ca2+ in monolayers and suspensions of various types of animal cells. *The Journal of cell biology* **105,** 2145-2155.

Maskell P. D., Speder P., Newberry N. R. and Bermudez I. (2003) Inhibition of human alpha 7 nicotinic acetylcholine receptors by open channel blockers of N-methyl-D-aspartate receptors. *British journal of pharmacology* **140,** 1313-1319.

McDonough J. H., Jr. and Shih T. M. (1993) Pharmacological modulation of soman-induced seizures. *Neuroscience and biobehavioral reviews* **17,** 203-215.

McShane R., Areosa Sastre A. and Minakaran N. (2006) Memantine for dementia. *Cochrane database of systematic reviews* CD003154.

Minta A., Kao J. P. and Tsien R. Y. (1989) Fluorescent indicators for cytosolic calcium based on rhodamine and fluorescein chromophores. *The Journal of biological chemistry* **264,** 8171-8178.

Motulsky H. and Christopoulos A. (2003) *Fitting models to biological data using linear and non -linear regression. A practical guide to curve fitting.* GraphPad Software Inc., San Diego, CA.

Nedergaard M., Ransom B. and Goldman S. A. (2003) New roles for astrocytes: redefining the functional architecture of the brain. *Trends in Neurosciences* **26,** 523-530.

Negulescu P. A. and Machen T. E. (1990) Intracellular ion activities and membrane transport in parietal cells measured with fluorescent dyes. *Methods in enzymology* **192,** 38-81.

Neher E. (1989) Combined fura-2 and patch clamp measurements in rat peritonial mast cells, in *Neuromuscular Junction* (Sellin L. C., Libelius R. and Thesleff S., eds), pp 65-76. Elsvier, Amsterdam.

Oliver A. E., Baker G. A., Fugate R. D., Tablin F. and Crowe J. H. (2000) Effects of temperature on calcium-sensitive fluorescent probes. *Biophysical journal* **78,** 2116-2126.

Olsen R. W. and Betz H. (2006) GABA and Glycine, in *Basic Neurochemistry,* 7th Edition (Siegel G. J., Albers R. W., Brady S. T. and Price D. L., eds), pp 291-301. Elsvier Academic Press, London.

Parekh A. B. and Putney J. W., Jr. (2005) Store-operated calcium channels. *Physiological reviews* **85,** 757-810.

Parsons C. G., Danysz W. and Quack G. (1999) Memantine is a clinically well tolerated N-methyl-D-aspartate (NMDA) receptor antagonist--a review of preclinical data. *Neuropharmacology* **38,** 735-767.

Peng X., Katz M., Gerzanich V., Anand R. and Lindstrom J. (1994) Human alpha 7 acetylcholine receptor: cloning of the alpha 7 subunit from the SH-SY5Y cell line and determination of pharmacological properties of native receptors and functional alpha 7 homomers expressed in Xenopus oocytes. *Molecular pharmacology* **45,** 546-554.

Peng X., Gerzanich V., Anand R., Wang F. and Lindstrom J. (1997) Chronic Nicotine Treatment Up-Regulates alpha 3 and alpha 7 Acetylcholine Receptor Subtypes

Expressed by the Human Neuroblastoma Cell Line SH-SY5Y. *Molecular pharmacology* **51,** 776-784.

Petr M. J. and Wurster R. D. (1997) Determination of in situ dissociation constant for Fura-2 and quantitation of background fluorescence in astrocyte cell line U373-MG. *Cell Calcium* **21,** 233-240.

Picciotto M. R. (2003) Nicotine as a modulator of behavior: beyond the inverted U. *Trends in pharmacological sciences* **24,** 493-499.

Price G. W., Ahier R. G., Middlemiss D. N., Singh L., Tricklebank M. D. and Wong E. H. (1988) In vivo labelling of the NMDA receptor channel complex by [3H]MK-801. *European journal of pharmacologyl* **158,** 279-282.

Rang H. P., Dale M. M., Ritter J. M. and P.K.Moore (2003) *Pharmacology,* 5th Edition. Churchill Livingstone, London.

Raveh L., Weissman B. A., Cohen G., Alkalay D., Rabinovitz I., Sonego H. and Brandeis R. (2002) Caramiphen and scopolamine prevent soman-induced brain damage and cognitive dysfunction. *Neurotoxicology* **23,** 7-17.

Raveh L., Brandeis R., Gilat E., Cohen G., Alkalay D., Rabinovitz I., Sonego H. and Weissman B. A. (2003) Anticholinergic and antiglutamatergic agents protect against soman-induced brain damage and cognitive dysfunction. *Toxicological sciences* **75,** 108-116.

Reisine T. and Pasternak G. (1995) Opioid analgecics and antagonists, in *Goodman & Gilman's The Pharmacological Basis of Theraputics,* 9th Edition, pp 503-519. McGraw-Hill, New York.

Ross R. A., Spengler B. A. and Biedler J. L. (1983) Coordinate morphological and biochemical interconversion of human neuroblastoma cells. *Journal of the National Cancer Institute* **71,** 741-747.

Runden-Pran E., Tanso R., Haug F. M., Ottersen O. P. and Ring A. (2005) Neuroprotective effects of inhibiting N-methyl-d-aspartate receptors, P2X receptors and the mitogen-activated protein kinase cascade: A quantitative analysis in organotypical hippocampal slice cultures subjected to oxygen and glucose deprivation. *Neuroscience* **136,** 795-810.

Shaw P. J. (2005) Molecular and cellular pathways of neurodegeneration in motor neurone disease. *Journal of neurology, neurosurgery, and psychiatry* **76,** 1046-1057.

Sheridan R. D., Smith A. P., Turner S. R. and Tattersall J. E. (2005) Nicotinic antagonists in the treatment of nerve agent intoxication. *Journal of the Royal Society of Medicine* **98,** 114-115.

Shih T.-M., McDonough J. H. and Koplovitz I. (1999) Anticonvulsant for Soman-Induced Seizure Activity. *Journal Biomedical Science* **6,** 86-96.

Silver I. A. and Erecinska M. (1990) Intracellular and extracellular changes of [Ca2+] in hypoxia and ischemia in rat brain in vivo. *The Journal of general physiology* **95,** 837-866.

Sokolova E., Matteoni C. and Nistri A. (2005) Desensitization of neuronal nicotinc receptors of human neuroblastoma SH-SY5Y cells during long or short exposure to nicotine. *British Journal of Pharmacology* **146,** 1087-1095.

Solberg Y. and Belkin M. (1997) The role of excitotoxicity in organophosphorous nerve agents central poisoning. *Trends in Pharmacological Sciences* **18,** 183-185.

Standaert D. G. and Young A. B. (1995) Treatment of Central Nervous System Degenerative disorders, in *Goodman & Gilman's The Pharmacological Basis of Theraputics,* 9th Edition, pp 503-519. McGraw-Hill, New York.

Syvälahti E. K. G., Kunelius R. and Laurén L. (1988) Effects of Antiparkisonian Drugs on Muscarinic Receptor Binding in Rat Brain, Heart and Lung. *Pharmacology & Toxicology* **62,** 90-94.

Tattersall J. E. (1993) Ion channel blockade by oximes and recovery of diaphragm muscle from soman poisoning in vitro. *British journal of pharmacology* **108,** 1006-1015.

Taylor P. (1995) Anticholinesterase agents, in *Goodman & Gilman's The Pharmacological Basis of Theraputics,* 9th Edition (Hardman J. G., Limbird L. E., Molinoff P. B., Ruddon R. W. and Gilman A. G., eds), pp 161-176. McGraw-Hill, New York.

Taylor P. and Brown J. H. (2006) Acetylcholine, in *Basic Neurochemistry,* 7th Edition (Siegel G. J., Albers R. W., Brady S. T. and Price D. L., eds), pp 185-209. Elsevier Academic Press, London.

Timperley C. M., Bird M., Heard S. C., Notman S., Read R. W., Tattersall J. E. H. and Turner S. R. (2005) Fluorinated pyridine derivatives: Part 1. The synthesis of some mono- and bis-quaternary pyridine salts of potential use in the treatment of nerve agent poisoning. *Journal of Fluorine Chemistry* **126,** 1160-1165.

Tsien R. Y. (1981) A non-disruptive technique for loading calcium buffers and indicators into cells. *Nature* **290,** 527-528.

Tsien R. Y. and Harootunian A. T. (1990) Practical design criteria for a dynamic ratio imaging system. *Cell Calcium* **11,** 93-109.

Tsien R. Y., Rink T. J. and Poenie M. (1985) Measurement of cytosolic free Ca2+ in individual small cells using fluorescence microscopy with dual excitation wavelengths. *Cell Calcium* **6,** 145-157.

van Helden H. P. M. and Bueters T. J. H. (1999) Protective activity of adenosine receptor agonists in the treatment of organophosphate poisoning. *Trends in Pharmacological Sciences* **20,** 438-441.

Vander A., Sherman J. and Luciano D. (2001) *Human Physiology, the mechanisms of body function,* 8th Edition. McGraw-Hill Book Co, Singapore.

Wolff C., Fuks B. and Chatelain P. (2003) Comparative study of membrane potential-sensitive fluorescent probes and their use in ion channel screening assays. *Journal of biomolecular screening* **8,** 533-543.

Wong E. H. F., Kemp J. A., Priestley T., Knight A. R., Woodruff G. N. and Iversen L. L. (1986) The Anticonvulsant MK-801 is a Potent N-methyl-D-aspartate Antagonist. *Proceedings of the National Academy of Sciences of the United States of America* **83,** 7104-7108.

Yokogawa K., Nakashima E., Ishizaki J., Hasegawa M., Kido H. and Ichimura F. (1992) Brain regional pharmacokinetics of biperiden in rats. *Biopharmaceutics & drug disposition* **13,** 131-140.

Aas P. (2003) Future considerations for the medical management of nerve-agent intoxication. *Prehospital and disaster medicine* **18,** 208-216.

Aasly J. O. (2004) T 6.3.4 Anitkolinergika, in *Norsk Legemiddelhåndbok* (Vilberg A., ed.). Foreningen for utgivelse av Norsk legemiddelhåndbok, Oslo.